EUR 4053 e

EUROPEAN ATOMIC ENERGY COMMUNITY — EURATOM

GAMMA PHASE URANIUM-MOLYBDENUM FUEL ALLOYS

by

G. BEGHI

1968

Joint Nuclear Research Center
Ispra Establishment — Italy

Metallurgy and Ceramics

LEGAL NOTICE

This report is on sale at the addresses listed on cover page 4

at the price of FF 12.50	FB 125.—	DM 10.—	Lit. 1 560	Fl. 9.—

When ordering, please quote the EUR number and the title, which are indicated on the cover of each report.

Printed by Van Muysewinkel
Brussels, September 1968.

EUR 4053 e

GAMMA PHASE URANIUM-MOLYBDENUM FUEL ALLOYS by G. BEGHI

European Atomic Energy Community — EURATOM
Joint Nuclear Research Center — Ispra Establishment (Italy)
Metallurgy and Ceramics
Brussels, September 1968 — 82 Pages — 53 Figures — FB 125

Available information on the gamma phase uranium-molybdenum alloys, mainly the U-10 wt% Mo alloy, are summarized; the bibliographic review includes data up to 31.12.1967.

The characteristics reported are :

— gamma stability : thermal transformation kinetics (TTT diagrams) of the metastable gamma phase;
— dimensional stability under thermal cycling and under irradiation — several irradiations experiments are reported, with the results related to radiation induced phase reversal and swelling;
— physical and mechanical properties as determined by different authors.

EUR 4053 e

GAMMA PHASE URANIUM-MOLYBDENUM FUEL ALLOYS by G. BEGHI

European Atomic Energy Community — EURATOM
Joint Nuclear Research Center — Ispra Establishment (Italy)
Metallurgy and Ceramics
Brussels, September 1968 — 82 Pages — 53 Figures — FB 125

Available information on the gamma phase uranium-molybdenum alloys, mainly the U-10 wt% Mo alloy, are summarized; the bibliographic review includes data up to 31.12.1967.

The characteristics reported are :

— gamma stability : thermal transformation kinetics (TTT diagrams) of the metastable gamma phase;
— dimensional stability under thermal cycling and under irradiation — several irradiations experiments are reported, with the results related to radiation induced phase reversal and swelling;
— physical and mechanical properties as determined by different authors.

EUR 4053 e

EUROPEAN ATOMIC ENERGY COMMUNITY — EURATOM

GAMMA PHASE URANIUM-MOLYBDENUM FUEL ALLOYS

by

G. BEGHI

1968

Joint Nuclear Research Center
Ispra Establishment — Italy

Metallurgy and Ceramics

Summary

Available information on the gamma phase uranium-molybdenum alloys, mainly the U-10 wt% Mo alloy, are summarized; the bibliographic review includes data up to 31.12.1967.

The characteristics reported are :

— gamma stability : thermal transformation kinetics (TTT diagrams) of the metastable gamma phase;

— dimensional stability under thermal cycling and under irradiation — several irradiations experiments are reported, with the results related to radiation induced phase reversal and swelling;

— physical and mechanical properties as determined by different authors.

KEYWORDS

URANIUM ALLOYS
MOLYBDENUM ALLOYS
PHASE DIAGRAMS
BIBLIOGRAPHY
PHASE TRANSFORMATION
STABILITY
THERMAL CYCLING
RADIATION EFFECTS
SWELLING
MECHANICAL PROPERTIES

TABLE OF CONTENTS

LIST OF TABLES

LIST OF FIGURES

1. INTRODUCTION (*)

Dimensional stability of fuel elements during extended reactor exposure is one of the most important and difficult technical problems in nuclear technology.
This property, that is, high resistance to growth and swelling, is sensitive to the metallurgical structure of the material.

Uranium exists in three allotropic forms: alpha (orthorhombic) below 661°C; beta (tetragonal) between 661 and 769°C; and gamma (body centered cubic) from 769°C to the melting point (1130°C) (1). Research on satisfactory uranium alloys has been made in two principal directions:

a) alloy additions in relatively low concentrations. Additions are normally designed to yield a structure combining random orientation and fine grain size. These alloys are best suited for the utilization of natural or slightly enriched uranium in thermal reactors.

b) alloy additions in sufficient concentrations to stabilize partially or completely the cubic gamma phase, thereby circumventing the intrinsic instability of the orthorhombic alpha structure. The resulting alloys may be referred to as "gamma phase alloys"; they are most suitable for fast reactors since they require higher contents of alloying additions.

Considerable effort has been expended on the development of metastable gamma phase uranium alloys with molybdenum; particularly much work has been done on the U-10 wt% *) Mo alloy because of its high strength, stability, homogeneity and ease of fabrication.

This well known gamma phase uranium alloy, in the range 9-10% Mo, was chosen as initial fuel material for SORA (2). This alloy was previously selected for the Dounreay Fast Reactor, the Enrico Fermi Fast Reactor, the

---

*) Composition will be specified as wt% throughout this paper.

(*) Manuscript received on May 22, 1968.

Hallam Nuclear Power Facility and several fast burst reactors (Oak Ridge HPRR, White Sands Molly G, Lawrence Laboratory Super Kukla, and Sandia APRFR).

Information on this alloy is summarized in this paper; the characteristics considered are:

a) gamma stability: transformation kinetics of the metastable gamma phase;

b) dimensional stability under thermal cycling and under irradiation;

c) physical and mechanical properties.

These are the basic properties which must be considered for the selection of the uranium alloy best-suited for the requirements of SORA reactor.

2. TRANSFORMATION KINETICS OF THE METASTABLE GAMMA PHASE

Dimensional stability is related to the ability to retain the gamma phase in metastable equilibrium: uranium molybdenum alloys are interesting because of the sluggishness with which the isotropic gamma phase transforms at low temperatures.

Uranium molybdenum has been the most widely studied system of the U alloys. Studies prior to 1958 were summarized by ROUGH and BAUER (3): the equilibrium diagram is reproduced as fig. 1. The most authoritative version of the diagram up to 900°C is that of DWIGHT (4): fig. 2.

The uranium-molybdenum system is one of the few uranium alloy systems which have extensive solid solution in the gamma phase: U-Nb, U-Zr, U-Ti, U-Mo, U-V (5). At 560°C the gamma phase undergoes an eutectoid decomposition $\gamma \rightarrow \alpha + \gamma'$ (6) (γ' is also referred to as δ or ε). A certain amount of molybdenum (up to about 1%) can be dissolved in the α phase of uranium (7). The γ' phase, having the approximate composition of UMo_2, has a tetragonal structure (7)(8). The unit cell of this phase is a vertically tripled γ uranium cell; the positions of the atoms in the γ' phase lattice

correspond to an ordered arrangement of uranium and molybdenum atoms.

The gamma phase may be retained at room temperature by quenching, or even slow cooling, from the gamma region for alloys having from 5.4 to approximately 20 wt% Mo, the limit of solid solubility of molybdenum in gamma uranium (9). Heat treating in the γ' phase region results in transformation of the gamma phase, but the transformation occurs very slowly.

Transformation kinetics have been studied early in an exploratory manner; detailed studies have been performed only in the most recent investigations.

SALLER, ROUGH and BAUER (10) (1954) studied 10-25 wt% Mo alloys indicating only the times for the initiation of transformation. They concluded that the transformation of gamma is sluggish at all temperatures, the rate decreases rapidly below 440°C and the nose of the C-curve lies close to 500°C.

The isothermal decomposition of five gamma phase alloys with molybdenum content ranging from 7 to 12 w/o was studied by McGEARY (11) (1955); times for beginning of transformation were determined: fig. 3.

Transformation kinetics of uranium-base alloys containing 5.4, 8, 10 and 12 wt% molybdenum were investigated by VAN THYNE and McPHERSON (12) (1957). The curve of initial decomposition has been shown on the TTT diagrams, determined by different techniques: fig. 4 and 5. For any given alloy and temperature the observed times for transformation vary, depending upon the techniques employed (fig. 6); however, using any given technique trends due to alloying are similar.

A TTT diagram for a U-8 % Mo alloy was determined from dilatometry by BELLOT, DOSIERE and HENRY (13) (1958) at higher temperatures: fig. 7.

The mode of transformation to the stable phase, alpha uranium, and to the ordered phase γ' vary considerably depending on temperature of annealing and molybdenum content.

In a study of the decomposition mechanism of the gamma phase, DONZE and CABANE (14) (1960) have published a TTT diagram for the beginning of transformation in a uranium alloy with ~8% Mo: fig. 8.

MIKHAILOFF (15) has studied (1960) the transformation mechanisms at low temperature and at higher temperatures in 6 and 10 wt% Mo alloys. For the alloy containing 10 wt% molybdenum the return to the equilibrium state follows two types of reaction:

- pearlite transformation by nucleation and growth from the grain boundaries, preponderant when the annealing takes place at temperatures above 400°C;
- transformation inside the grains of the quenched solid solution; at 400°C or below, with formation of small ordered regions and then a fine α phase precipitate.

No TTT diagram with specified times of transformation was published.

In a study of isothermal transformation kinetics at 550°C of U-14 and U-16 w/o Mo alloys, HOLLAND shows (16) (1961), with data obtained also by different authors, that U-10 w/o Mo alloys are more gamma stable at 550°C than other alloys in the range of about 5 to 16 % Mo (fig. 9).

SHOUDY, McHUGH and SILLIMAN (17) (1962) have published a metallographically determined TTT curve for a U-10 w/o Mo fabricated into fuel pins. Times were indicated for 50% transformed ($\alpha + \delta + \gamma$) alloy and 100% transformed ($\alpha + \delta$) alloy: fig. 10.

A study on the influence of alloying on the isothermal TTT characteristics of uranium alloys was published by PETERSON, STEELE and DIGIALLONARDO (18) (1964). For temperatures below 450°C it is only reported that no evidence is found of gamma phase transformation until the elapse of considerable time.

The kinetics of gamma decomposition in a U-10.8 wt% Mo were studied also by BAR-OR et al. (19) (1964). The two determined TTT curves are re-

presented in fig. 11: at 550°C the $\gamma \rightarrow \alpha + \gamma'$ transformation proceeds directly, while at and below 500°C the $\alpha + \gamma'$ is preceded by the appearance of $\alpha + \gamma$.

REPAS, GOODENOW and HEHEMANN (20) (1964) have studied both the high and low temperature decomposition processes in two binary gamma-phase uranium alloys: 8 and 10% molybdenum. They presented complete TTT diagrams based on metallographic, dilatometric, microhardness and X-ray diffraction data: fig. 12, 13. As illustrated in these diagrams, the decomposition of the metastable gamma phase is relatively complex and takes place by several different mechanisms. In the high temperature range (above approximately 375°C) a cellular type discontinuous precipitation is observed as well as the precipitation of Widmanstätten alpha. The equilibrium γ' phase is not precipitated initially but develops within the cellular structure on continued isothermal holding.
Transformation at temperatures below approximately 375°C involve a different mechanism or mechanisms. Decomposition initiates by precipitation of γ' which bears a discrete lattice relationship with the γ matrix; subsequently, α is precipitated also with a lattice relationship to γ.

Another work published in 1967 by GOLDSTEIN and BAR-OR (21) indicates TTT curves for uranium alloys with 8 wt% and 10.8 wt% molybdenum: fig. 14. The authors worked with powder, not with massive samples. Below 550°C for the U-8 wt% Mo (below 500°C for the 10.8% alloy) a gradual transformation, first to the ($\alpha + \gamma$) phase and then to the ($\alpha + \gamma + \gamma'$) phase, occurred.
No significant effect of impurities on the TTT curves was found.

3. THERMAL CYCLING

During thermal cycling of polycrystalline uranium, changes in structure and dimensions may occur.
These changes, which depend strongly on both the thermal mechanical history of the metal and the exact time-temperature schedule of each thermal cycle, may show as surface roughening, increase or decrease in dimensions,

porosity, and changes in microstructure.

Much work has been published concerning these effects in uranium. In general, the addition of alloy elements decreases the magnitude of this problem, but nevertheless it should be investigated for each new uranium alloy, contemplated for reactor use.

a) Thermal cycling tests on U-9.36 wt% Mo alloy have been reported by SALLER et al. (22) (1956). Specimens in both gamma and the alpha plus delta condition, were examined after 530 cycles between 150°C and 725°C. All the specimens appeared little affected and possessed smooth surfaces and a good appearance. The change in length and diameter was less than 0.1% per 100 cycles. The possibility exists that the specimens initially heat treated to transform γ to $\alpha + \delta$ had reverted to gamma phase during thermal cycling above the gamma transformation temperature (575°C). If this had occurred, the reported results would be valid only for gamma U-10 wt% Mo.

b) In the Enrico Fermi (EFFBR) Program, experiments have been conducted at the Detroit Edison Engineering Research Laboratory to determine the effect of thermal cycling on U-10 wt% Mo fuel pin samples (23) (24).
The specimens were placed in vycor capsules which were filled with a partial pressure of argon. The capsules containing the specimens were placed in a resistance heated furnace and cooled by an air line.
A test was made with a transformed (alpha plus epsilon) fuel pin to determine whether these specimens cycled in the alpha plus epsilon phase would exhibit dimensional instability.
The fuel pin used in this experiment was transformed from gamma to alpha plus epsilon by heating to 475°C for 180 hours in vacuum. The specimens were thermally cycled between room temperature and 525°C for 504 cycles. Heating required about 15 min, cooling was accomplished in 4 min.
The physical dimensions of all the samples were altered slightly as a result of the thermal cycle tests. The maximum dimensional changes were + 0.3% in diameter and -0.1% in length. The metallographic changes also

appear to be of a low order of magnitude: only a slight coarsening of the alpha plus epsilon structure occurred.

c) In the experimental program for the ORNL Health Physics Research Reactor (HPRR) Design thermal cycling tests on U-10 wt% Mo alloy were performed (25) (1960). Encapsulated specimens were plunged into a 760°C furnace and heated to the upper cycle temperatures. The specimens were then withdrawn from the furnace and allowed to cool to about 60°C in 15 or 20 min before repetition of the cycle. The heating rate was essentially constant at 215°C/min up to about 500°C and departed from a linear rate above that temperature. The average rate for specimens heated to 680°C was ~150°C/min. About 1000 thermal cycles of the U-10 wt% Mo pins, either within the gamma metastable range (565°C and 515°C) or into the gamma range (680°C), did not cause significant changes in density, length or diameter of either retained gamma or partially transformed (~20%) pins. It appears that although transformation can be initiated during thermal cycling, as far as distortion or growth of fuel is concerned, there are no serious consequences even if the fuel should partially transform to $\alpha + \delta$.

The author emphasizes that although results are very encouraging, the limitation in applying them to the ORNL Fast Burst Reactor should be apparent. The thermal cycle associated with operation of the ORNL HPRR involves extremely rapid (~40 microsecond) heating of the fuel, followed by relatively slow cooling to room temperature. Rapid heating produces large inertial stresses. The possibility of reproducing the rapid heating and consequent inertial stresses was considered but was not pursued because of the complexity and cost of the experiment.

The thermal cycle tests that were performed simulated the total time at temperature for typical portions of fuel and provided information on thermal cycling distortion and transformation in the absence of inertial stresses.

4. IRRADIATION STABILITY

The irradiation performance of a fuel depends upon a complex interrelation of several variables, each of which plays a significant role.

The use of uranium alloys is limited by the dimensional changes in the material during reactor operation; the main sources of this dimensional instability are fission event damage and fission product damage.

Fission event damage:
The kinetic energy of the fission-product atoms is dissipated by interactions and collison with both electrons and atoms. The collisions with the lattice atoms give rise to displacements of atoms, resulting in the formation of vacancies, interstitial atoms and displacement spikes. Among the principal displacement phenomena observed in fissionable materials are:

a) anisotropic growth of uranium and uranium rich alpha-phase alloys;

b) phase reversal in uranium alloys.

The term "anisotropic growth" describes the change in shape which occurs under irradiation; it is not necessarily accompanied by an increase in volume. Several theoretical mechanisms have been proposed to account for the growth of alpha uranium under irradiation (25).
These are of two main types: the first is based on the anisotropic diffusion of the interstitials and vacancies produced by the fission fragments, and the second is based on the local expansion produced by the fission spike.

"Phase reversal" refers to an atomic-displacement phenomenon that results in a transformation from a stable to a metastable phase by neutron bombardment. The phenomenon of phase reversal was independently reported by KONOBEEVSKY et al. (27) (28) and by BLEIBERG et al. (29) (30) for uranium-molybdenum and uranium-niobium alloys. In both experiments it was observed that a transformed sample of U-10 wt% Mo consisting of alpha plus epsilon and alpha plus gamma, respectively, reverted to the metastable gamma phase after neutron irradiation. The tendency towards equilibrium, alpha plus epsilon, the epsilon or γ' being the ordered form of the gamma

phase, is opposed by the effect of irradiation, which causes a reversal of the transformation reaction by localized thermal agitation of the alloy and reforming the high temperature epsilon phase.

Fission product damage: commonly referred to as swelling.
This term refers to that form of dimensional instability of materials caused by the formation of fission products and, in particular, of gas bubbles containing the inert-gas fission products, xenon and krypton.

Other sources of dimensional instability in reactor fuel-elements are cracking, void formation, expansion or contraction due to phase changes, thermal stresses, thermal shock, and creep.

The phenomena due to irradiation induce two coexistent dimensional effects in uranium alloys:

1) anisotropic or "plastic" growth, with little change in density;
2) the increase of all dimensions concurrently, as evidenced by a density decrease (referred to as "volume change").

a) Early studies on the irradiation behaviour of uranium alloys indicated that the alloy which possessed the best comportement was the U-10 wt% Mo alloy: some results were reported in (31)+ (34).

b) The investigations exposed by LEESER et al. (34) (1958) indicated a good radiation stability of gamma treated 10 wt% Mo material to 2 at % burn-up at fuel temperatures below to 600 $\pm$ 90°C.
No significant effect of composition variations between 9 and 11 wt% Mo was noted.

c) In the program of alloy development for the Pressurized Water Reactor, Westinghouse investigated radiation stability of several binary uranium alloys. The results have benn summarized in a WAPD report (35) (1957).
Both zircaloy-2-clad and unclad alloys were irradiated in the MTR; the U-Mo alloys investigated were U-9 wt% Mo, U-10.5 wt% Mo, U-12 wt% Mo, U-13.5 wt% Mo.

The unclad specimens irradiated in NaK-filled capsules showed no measurable changes in dimensions and density for gamma-quenched U-Mo alloys exposed to less than 1200 MWD/T. For higher exposure, comparison of the changes in diameter and length indicated no appreciable anisotropic growth, since the percent increase in both was approximately equivalent. The density decreases of gamma-quenched U-10.5 - 12 and 13.5 wt% Mo alloys versus exposure are plotted in fig. 15. Because of the scatter in the data, any effects of molybdenum content on density change are inconclusive. The surface of the samples did not show any signs of roughening, although a slight bow distortion did occur in the highest exposure samples. The samples were very brittle.

It may be concluded from the data that gamma-phase alloys irradiated at central temperatures of less than 400°C decrease in density about 0.5% per 0.1 a/o burn-up (1000 MWD/T) for burn-ups to approximately 0.8 a/o.

Uranium-molybdenum specimens clad in zircaloy-2 also increased in dimensions with increasing exposure. Samples irradiated in the gamma-quenched condition showed no significant changes in dimensions when exposed to 5610 MWD/T or less. This is to be compared with density decrease of about 3% for unclad gamma-quenched material given a similar exposure. The maximum volume increase of 4.3% occurred at an exposure of 28,000 MWD/T and caused the cladding to split.

Fig. 16 summarizes irradiation data for a series of alloys of the Westinghouse experiments (most of them contain molybdenum).
Use of a cladding markedly diminishes volume changes; it was concluded that much of the volume change, in gamma phase alloys, is probably due to formation of voids which may be suppressed, at least at the surface, by cladding.
Westinghouse data has also shown that at low temperature (less than 250°C) and low burn-up, the alpha plus delta phase reverts to the gamma phase while the gamma phase remains essentially unchanged.

Subsequent to the early irradiation tests, extensive evaluations of U-10 Mo

alloy have shown this alloy to be sensitive to radiation and thermal conditions. Under certain conditions of fission rate and temperature, this alloy distorts severely.

d) A complete summary of the available data, in 1960, on U-10 wt% Mo alloy was given by A. BOLTAX (25): the maximum central temperature, measured density decrease and total burn-up are given in fig. 17. In the gamma phase alloys (> 7.5 wt% Mo) the irradiation stability is dependent on the phase-reversal phenomenon, which would not be expected to be sensitive to pre-irradiation history as long as the critical flux necessary to maintain the alloy in the gamma phase were exceeded.
However, heat treatment can affect the alpha plus epsilon lamella spacing and may cause a change in critical flux.
The data of fig. 17, replotted in fig. 18 and 19, show the phenomenon of abnormal swelling in the narrow temperature range of 335-390°C. This abnormal swelling is associated with the competitive processes of phase reversal (alpha plus epsilon to gamma) and thermal decomposition of the gamma phase (gamma to alpha plus epsilon). At high burn-up rates the gamma phase is stable at all temperatures, but at low burn-up rates there may be a narrow temperature range wherein thermal decomposition occurs rapidly enough to lead to the abnormal swelling.

The uranium 10 wt% Mo fuel alloy was selected for the first core loading in the Enrico Fermi Fast Breeder Reactor in 1956. In the fuel development program, irradiations and studies were performed by Atomic Power Development Associates (APDA) and Battelle Memorial Institute (BMI).

e) A first irradiation program was accomplished in the Materials Testing Reactor (MTR) at high fission rates. The results have been reported: (33) (36) (37) (38). Shown in fig. 20 is the density decrease versus burn-up for the U-10 wt% Mo alloy. A solid curve which extends to 2.0 at % burn-up has been drawn to incorporate the vast majority of points. The straight lines indicate a swelling rate of about 3% for at % burn-up. Indicated on the curve are the irradiation temperatures that were in excess of 480°C (900°F). Fig. 21 shows the density change for at % burn-up versus the

centerline irradiation temperature. Curves showing diameter changes as a function of burn-up and irradiation temperature are shown in fig. 22 and 23.

The following conclusions may be drawn from the results obtained during this phase of the MTR experiments:

1) The critical centerline irradiation temperature above which U-10 wt% Mo alloy swelled abnormally was in the range of 600°C. There was some indication that specimens would not swell abnormally at temperatures over 600°C, but only if the burn-up was below about 0.5 total at %.

2) The U-10 wt% Mo alloy swells linearly with increasing burn-up, at a rate of about 3.0 percent per at % burn-up, at irradiation temperatures below 540°C if transformation of the gamma phase does not occur during irradiation. This corresponds to a diameter increase of about 1.3 percent at % burn-up. It should be noted that there was some indication that the rate of increase in diameter might become more rapid at burn-ups above about 1.8 at %.

3) The gamma phase of the U-10 wt% Mo alloy was normally maintained during irradiation at fission rates in the range of 0.70×10^{14} f/cm^3-sec at temperatures below 540°C and at burn-ups under 2.7 at %.

4) The alloy exhibits a critical temperature, above which abnormal swelling is observed. Swelling is attributed to increased mobility of fission-gas atoms and decreased mechanical strength with increasing temperature.

5) Metallographic studies indicated that irradiation did not affect the microstructure of the alloy.

6) The data did not indicate any significant effect of heat treatment prior to irradiation on the stability of the alloy during irradiation, so long as the alloy was in and remained in the gamma phase.

f) In a separate phase of the same program, fuel pins were irradiated in the CP-5 reactor at fission rates and central temperatures that would simu-

late those to be expected in the Fermi reactor (38) (39). The MTR and CP-5 data below 600°C were correlated in fig. 24 as a plot of percent diameter increase per atom percent burn-up versus temperature. Large disparity was found between the CP-5 results and the remainder of the data in the range of 400°C to 600°C. An explanation of this difference has been discussed on the basis of three hypotheses (transformation effect, thermal cycling effects, internal defects); the most plausible theory was considered the fission-rate effect.

g) At the "Symposium on Radiation Damage in Solids and Reactor Materials", Venice 1962, SHOUDY, McHUGH and SILLIMAN (17) presented the results of an irradiation program initiated to investigate the effect of fission rate on the transformation kinetics and radiation stability of the Fermi Reactor production fuel pins.

Fig. 25 gives the diametral increase as a function of burn-up for the specimens irradiated in MTR, the data is plotted to indicate two separate fission rates and temperature ranges.
The following conclusions have been drawn for U-10 wt% Mo alloy.

- A fission rate of 3.6×10^{13} fissions/cm^3-sec is sufficient to maintain the gamma phase or cause the $\alpha + \gamma'$ phases to revert to gamma during irradiation at temperatures up to about 450°C. Under these conditions, the dimensional stability of the fuel is good for burn-ups to at least 1.0 at %.
- At temperatures between 500°C and 570°C a fission rate of at least 7×10^{13} fissions/cm^3-sec was required to maintain the gamma or to cause the $\alpha + \gamma'$ phases to revert to the gamma phase during exposures of up to ~ 1.0 at % burn-up.
- At a fission rate less than 6×10^{13} fissions/cm^3-sec and irradiation temperature of 480° - 565°C, the diameter changes become increasingly larger for decreasing fission rates. Post-irradiation examination has shown that the loss of dimensional stability can be related to the transformation kinetics of the fuel alloy while under irradiation. At high fission rates, the metastable gamma phase continues to exist, and the diameter changes are small and relatively insensitive to burn-up. At progressively lower fission

rates, the alloy transforms partially or completely to the equilibrium alpha plus delta phases, the degree of transformation depending on the absolute fission rate and the radiation temperature. Under these conditions, diameter increases for burn-ups of about 1 at % range from 3 to 14% for fission rates of 5×10^{13} to 2×10^{13} fissions/cm^3-sec, respectively, and are highly dependent on burn-up. In these conditions a linear dependence of swelling on fission rate is shown in fig. 26.

- The swelling characteristics during irradiation are only slightly influenced by the phases present in the alloy prior to irradiation.

h) Uranium-molybdenum binary alloys were studied by Atomics International as prospective fuel for Advanced Sodium Cooled Reactors (40). A series of experiments was designed to show the effect of molybdenum and the influence of burn-up on the dimensional changes taking place. The authors emphasized that, due to the complexity of the experiments and the interdependence of the many variables, great care must be taken in trying to isolate the effect of any particular variable. Also the common form of presentation, density change as a function of burn-up, is not as simple as it may seem. Not only burn-up, but also temperature is being taken into account, the temperature obtained is proportional to the total burn-up, and for different capsules there is a different correspondence between burn-up and temperature.

It is confirmed that the swelling resistance of uranium is markedly increased by molybdenum additions: fig. 27. For low burn-ups, there is little to be gained by further increases in alloying additions above 7 or 8 wt% Mo. At the higher level of burn-ups, however, there is a significant improvement gained by increasing the molybdenum content beyond 8%.

For all conditions, the swelling first increases slowly with increasing burn-up, but eventually a point is reached where rapid swelling occurs, for the 10% alloy it is at about 9000 MWd/MTU (fig. 28).

In fig. 29 swelling is plotted against temperature. The temperature effect is significant, but it has not been possible to separate this unequivocally

from the burn-up effect.
Although some specimens were in the gamma phase, no difference could be seen in the behaviour of these and those in the $\alpha + \gamma'$ phase.

i) U-9 wt% Mo alloy fuel elements have been used in the Dounreay Fast Reactor and the results up to 1964 have been reported by COTTRELL et al. (41); the fuel had been successfully taken to a burn-up of 1.2 at %; (later data 2.2 at %).

Density measurements on uncracked fuel pieces indicate that three temperature ranges of swelling exist. At 1% burn-up when the fuel centre temperature is approximately 600°C-650°C the volume change was 6%; at temperatures below 500°C the change was 2.5% for 1% burn-up; whilst at intermediate temperatures the changes were about 10% for 1% burn-up, fission rates above 7×10^{13} fissions/cm^3-sec.

The assessment of dimensional changes was complicated by the occurrence of cracking. This cracking which occurred at quite an early stage was not expected from the results of irradiating this type of alloy in a materials testing reactor. There are many factors which could cause or contribute to cracking, such as thermal stresses, notch brittleness, swelling stresses, transformation stresses. The authors believed that cracking may be a consequence of the fast fission flux environment. In a thermal materials testing reactor, the self-shielding effect in fissile specimens greatly reduces the fission flux, and hence the burn-up in the interior of the fuel beneath the surface. The higher burn-up at the surface leads to swelling which could produce compression stresses. In a fast reactor, the intensity of the fission flux through the fuel cross section is virtually unaltered. The central fuel achieves the same burn-up as that at the surface but is operating at a considerable higher temperature. Under these conditions, interior fuel swelling imposes tensile tresses on the outermost fuel. These stresses together with thermal stresses, will lead to cracking.

Although cracking has been extensive in many elements, it has not directly affected the performance of the fuel elements or led to any failure.

j) Always on the basis of the informations obtained in the Dounreay Fast Reactor, J. L. PHILLIPS (42) presented later (1965) an analysis of the swelling behaviour of the U-9 wt% Mo fuel. The swelling is shown as a function of burn-up (fig. 30) and, also in these experimental results, there are seen to be three apparently significant ranges of peak fuel temperature, namely low temperature (up to 500°C), transformation range (500°-565°C), and high temperature (565°-675°C).

The analysis of the results in this way is perhaps an over-simplification particularly when it is remembered that the quoted temperatures refer to the peak fuel temperature, the surface temperature being much lower. Each measured result is, therefore, an integrated effect over a range of temperatures, and the actual swelling is a compromise between that of the hotter central material and that of the restraining cooler surface layers. A reasonable interpretation of the temperature ranges shown is possible, however, as follows:

- Low temperature range. At low peak fuel temperatures i.e. below 425°C, the fuel remains completely in the gamma phase. At a temperature of 425°C, transformation commences and at a peak fuel temperature of 500°C, the fuel surface temperature is approaching the transformation temperature and hence the transformation boundary is nearing the fuel surface. It appears that although transformation has occurred in the centre of the fuel, restraint by the surface layers of swelling of the transformed material has been successful, and thus the overall swelling corresponds with that expected for low temperature gamma phase material.

- Transformation range. For a peak fuel temperature in the range 500°-565°C, complete transformation of the fuel section occurs and the swelling behaviour is then typical of completely transformed material. This range gives results in good agreement with APDA data for 10 w/o Mo alloy. Extrapolation of this line backwards, indicates a reduction in volume at zero burn-up indicating the magnitude of the density change upon transformation.

- High temperature range. At a peak fuel temperature of 675°C, the transformation boundary has moved out to the fuel surface, all the fuel material then being in the gamma phase. The swelling behaviour then represents the combination of swelling of transformed material virtually unrestrained at the surface and somewhat restrained in the central regions.

As reported in the early results by COTTRELL (41), cracking occurred in the fuel, no correlation was observed between cracking and phase transformation. It is believed that, because of the high temperature gradients, the centre of the fuel will be tending to swell at a greater rate than the surface layers, thus causing additional tensile stresses in the surface.

Some investigations have been carried out on the effects of variations in the molybdenum content: 11.8 wt% Mo alloy exhibited a slightly reduced swelling rate but a greater tendency to crack. Fuel containing 7 wt% Mo was attractive in that it permitted the introduction of more experimental irradiations, and the results of irradiation of such fuel alloy elements indicated no significant difference in irradiation behaviour as compared with the 9 wt% alloy over the range of burn-ups so far covered. Consequently, in 1964 the standard fuel in the Dounreay Reactor was changed to U-7% Mo.

k) Atomics International carried out a fuel irradiation program to investigate the behaviour of U-10 wt% Mo fuel for the Hallam Nuclear Power Facility (HNPF) Core I. The range of temperature and fission rate conditions in the HNPF are indicated in the fig. 31. The results of the NAA 47 Core I Evaluation Experiments have been reported by A. R. SCHMITT et al. (43). Each of the eight irradiation tests contained nine 0.5 - in. diameter, 2.0-in. long, cast U-10 Mo fuel specimens, NaK bonded in a double-walled stainless steel capsule. Initially the fuel specimens were either as cast, partially transformed ($\alpha + \gamma' + \gamma$) or homogenized (γ). The experiments were irradiated in the Materials Testing Reactor. Only the low burn-up specimens were relatively stable; most of the fuel specimens swelled, sometimes excessively. Although many factors may have contributed to the observed damage, it was attributed by the authors primarily to the effects of

in-pile phase transformation at fission rates insufficient to retain the metastable gamma phase. The disordered gamma phase material constantly reverts to $\alpha + \gamma'$; this continuous transformation probably promotes fission gas bubble growth and/or reduces the in-pile strength of the fuel to such an extent that extreme irradiation instability results.

Although much of the observed swelling was probably due to the nucleation and growth of fission gas bubbles, a significant amount of the observed volume change resulted from internal microcracking of the fuel material.

Influence of temperature, fission rate and burn-up on the irradiation stability was exposed.

- Average operating temperature. Since the stability of U-10 Mo appears to be highly sensitive to in-pile phase transformation, temperature and temperature fluctuations must be considered as important variables influencing the stability of the fuel. Although it would be useful to isolate the effects of temperature and describe dimensional increase as a function of average fuel temperature, the wide variations in operating temperatures which the fuel experienced during irradiation reduce the significance of average temperature as an independent variable. In addition, it is difficult to isolate the effects of temperature and fission rate. However, in evaluating the data, some general trends are evident.

  Below 425°C, the fuel apparently behaves in a stable manner, retaining or transforming to the gamma phase during irradiation.
  At fuel central temperatures from 425°C to 600°C and at fission rates $< 1 \times 10^{13}$ fissions/cm^3-sec, the fuel appears to be very instable, and it transforms to a two-phase structure during irradiation.
  At fuel central temperature >600°C, fuel stability may be slightly improved.

- Temperature variations. The NAA 47 fuel specimens were subjected to several hundred thermal cycles, due to MTR power fluctuations or scrams. These abrupt temperature changes which were as great as 500°C, probably have a deleterious effect on fuel stability. The rapid thermal stresses

induced by the cycling may have promoted both the surface and internal cracking which contributed to the observed dimensional changes of the fuel.

- Fission rate. Fission rate is an extremely critical parameter influencing swelling. All fuel irradiated at fission rate $< 1 \times 10^{13}$ fissions/cm^3-sec and temperature above ~420°C exhibited severe dimensional changes, and these changes were a factor of 2 or 3 greater than those noted in the previous APDA experiments. In general the metallography showed that fission rates $< 0.7 \times 10^{13}$ fissions/cm^3-sec were insufficient to retain the gamma phase between 450°C and 560°C. At temperatures below 400°C the gamma phase was maintained or formed at fission rates $> 0.2 \times 10^{13}$ fissions/cm^3-sec.

- Burn-up. Although some irregularities were noted, in general, fuel swelling appeared to increase with burn-up. Fig. 32 shows percent diameter change as a function of burn-up, while fig. 33 gives average percent dimensional change $[\ 2(\%\ \Delta\ D) + \%\ \Delta\ L\ ]\ /3$ as a function of burn-up. The following conclusions have been drawn:
  - at burn-up levels above 3000 to 4000 MWd/MTU, dimensional change increases rapidly with burn-up, at a linear rate of about 2.5 to 3.0% dimensional increase per 1000 MWd/MTU;
  - based on the data available, below 3000 to 4000 MWd/MTU swelling appears to be less severe. This second conclusion is drawn from both high and low temperature irradiation data.

Among the characteristics of the irradiation damage, it was noted that specimens which experienced phase transformations or specimens which experienced temperature excursions, exhibited irregular surface cracks. The cracking appeared to be more severe in specimens which were given a gamma heat treatment, prior to irradiation. Metallographic examination revealed extensive microscopic porosity. Much of the internal porosity consisted of intergranular cracks, which undoubtedly contributed to the observed volume changes of the fuel.

The pre-irradiation microstructure resulting from various heat treatments appeared to have no appreciable effect on the irradiation stability of the fuel,

this observation is in agreement with previous works.

Some of these results have been summarized in the fig. 34 (44).

1) In the same irradiation program of the HNPF, WILLARD and SCHMITT (45) discussed particularly the phase reversion. It is known that the retention of gamma U-10 Mo in an irradiation environment is dependent on temperature and fission rate (27) + (30).

At temperatures below the eutectoid transformation temperature of 570°C, the retained gamma phase will transform to the stable eutectoid transformation products of α and γ', according to the TTT relationship (Par. 2). At temperatures below the nose of this curve, the rate of transformation is mostly dependent on the diffusion of atoms to nucleation sites. This diffusion may be expressed by the classical equation

$$D_t = D_o \exp\left(-\frac{Q}{R\,T}\right)$$

where

D_t = thermal diffusion coefficient

D_o = diffusion constant

Q = activation energy

R = gas constant

T = absolute temperature

During irradiation, thermal diffusion, which is temperature dependent, tends to transform the γ phase to $\alpha + \gamma'$.

The fission phenomenon is responsible for another type of diffusion, caused by the displacement spike formed by the energetic particles after a fission event. BLEIBERG (46) has shown a proportionality between the radiation diffusion coefficient and the fission rate. The coefficient is expressed by the equation:

$$D_R = \frac{(D_R)_1}{(Bu)_1} \times Bu$$

where

D_R = radiation-induced diffusion coefficient

$(D_R)_1 = 1.4 \times 10^{-18} \pm 0.6 \times 10^{-18}$ cm^2/sec (ref. 46)

Bu = critical fission rate

$(Bu)_1 = 5.25 \times 10^{12}$ fissions/cm^3-sec (ref. 46)

Thus $$D_R = 2.67 \times 10^{-31} \times Bu \ (cm^2/sec)$$

When $D_T > D_R$, the thermal transformation phenomenon predominates, and the metastable structure will follow the expected decomposition to the thermally stable phases ($\alpha + \gamma'$). However, the rate of transformation will decrease from that given on TTT curve by an amount which depends on the relative values of D_t and D_R. If $D_R > D_t$ then the radiation effect predominates, and the metastable phase will either be formed or retained, depending on the initial structure. An equilibrium condition exists between the two methods of transformation when

$$D_t = D_R$$

Physically this means that, for any temperature, there is a fission rate (Bu, called the critical fission rate) at which no transformation would occur. From the written equations this rate is

$$Bu = \frac{D_o \exp\left(-\frac{Q}{RT}\right)}{2.67 \times 10^{-31}} \ (fissions/cm^3\text{-}sec)$$

With the data of Raiklen, WILLARD and SCHMITT (45) have expressed

$$Bu = 3.75 \exp\left(-\frac{24,600}{T}\right) \times 10^{28} \ (fissions/cm^3\text{-}sec)$$

The critical fission rates calculated using this equation are the following:

temperature (°C)	critical fission rate (fissions/cm^3-sec)
371	8.8×10^{11}
385	2.2×10^{12}
399	4.8×10^{12}
413	9.2×10^{12}

A curve representing these data is presented in fig. 35; several specimens of the NAA-47 experiment have been plotted in the same figure. The observed metallographic structures are in good agreement with the theoretical curve. The only deviation is the specimen 4-9-S: but this may be explained by a lower actual temperature than the calculated temperature, due to penetration of cracks by the NaK.

The theoretical curve of the critical fission rate is naturally influenced by the values of the thermal and radiation-induced diffusion coefficients. Accuracy in these data may affect greatly the curve: an example is given in Appendix B.

A linear relationship of swelling to burn-up in the range of 3000 to 12000 MWd/MTU is confirmed. Deviations are related to excessively high central temperature, 700 to 800°C and to intergranular cracking.

This cracking is attributed to:

- formation of voids along grain boundaries as a result of complex stress systems. These stresses are attributed to temperature gradients, thermal cycles and differential expansion due to different structures (γ and $\alpha + \gamma'$) present in the same slug;
- growth of these voids, probably enhanced by vacancy production and mobility due to lattice disturbance by the fission process;
- coalescence of the voids; cracks from a grain boundary join with cracks from another grain boundary.

m) As part of the development program for the HNPF, a partial prototype of a HALLAM Core I fuel element (SU-9) was fabricated and irradiated in the Sodium Reactor Experiment (SRE). The results have been reported by ARNOLD et al. (47).

The fuel element assembly was irradiated to a maximum burn-up of 5,300 MWd/MTU, at a peak fission rate of approximately 1.5×10^{13} fissions/cm^3-sec and a maximum central temperature near 650°C. The post-irradiation examination of the fuel rods showed a low fission gas release of 0.1% and fuel dimensional changes ranging from -0.2% to +2.2% with corresponding density decreases from 0.2% to 6.4%. A plot of the average dimensional change versus burn-up is given in fig. 36. The fuel slugs which had burn-up less

than 4000 MWd/MTU were in excellent condition with maximum dimensional changes of less than +0.6%. The limiting peak burn-up would probably not be reached until at least 6000 MWd/MTU. Fuel slugs with burn-ups greater than 4000 MWd/MTU had extensive surface cracking and greater fuel dimensional changes.
Metallographic examination of the fuel showed that the slugs which had experienced the extensive surface cracking had most of their structure transformed to the $\alpha + \gamma'$ phase. The structure of the fuel which had no surface cracking and small dimensional changes, was essentially in the gamma phase. It is reconfirmed that $\alpha + \gamma'$ phase material is significantly less stable in an irradiation environment than the material remaining in the γ phase. There was evidence that the fuel which operated at lower temperatures had been homogenized to the gamma phase as a result of fission events, the mechanism being the radiation induced phase reversion.

n) The results of irradiations of uranium-molybdenum alloys have been reported by DMITRIEV et al. (48) (1967). The samples, contained in steel capsules filled with NaK, were irradiated in the following conditions: temperature between 100 and 200°C, thermal neutrons density $1 \div 2 \times 10^{13}$ n/cm^2/sec, integral flux $0.5 \div 1 \times 10^{20}$ neutrons/cm^2.
External examination and control measurements showed no surface modification and insignificant changes of dimensions for the U-7% and U-9% Mo alloys; the density, within the limits of accuracy of measurements, was not changed (scatter of the data $\pm$ 0.05 g/cm^3).

A finely divided dispersion of second phase particles is effective in reducing swelling in alpha-phase uranium alloys (49). Krypton and xenon bubbles, produced when uranium is irradiated, nucleate preferentially at internal surfaces, e.g. on inclusions.
Since these bubbles are of submicron size, large volume changes do not occur. Their tendency to agglomerate is reduced by a high concentration of dispersed particles; the binding energy between the gas atoms and the particles immobilize the bubbles.
This concept was applied by KRAMER et al. (50) (51) to U-10% Mo alloys with

0.04 wt% Tin. It must be noted that irradiation of an alloy containing a precipitated phase may result in solution of the precipitates and in formation of additional precipitates; the alloys should be heat-treated to yield the maximum density of the irradiation-induced precipitates. The improved swelling resistance of the samples with fine dispersions results from the data reported in Table I. The results of irradiations of similar materials are summarized in fig. 37, which shows the improvement obtained from fine-particle-producing additives and increased molybdenum content.

5. PHYSICAL AND MECHANICAL PROPERTIES

5.1 Density

The density of gamma-quenched uranium-molybdenum alloys versus molybdenum content, from ref. (11) is reported in Table 2.
The density of gamma-quenched uranium - 10 wt% molybdenum versus temperature is reported in Table 3 (ref. 52).

5.2 Thermal conductivity

Thermal conductivity values between 10°C and 100°C, reported by WESTINGHOUSE (11), are the following:

for U - 8 wt% Mo	0.034 ± 0.001 cal/(sec-cm^2-°C/cm)
for U - 12 wt% Mo	0.033 ± 0.001 cal/(sec-cm^2-°C/cm)

Thermal conductivity data versus temperature are represented in Table 4: APDA data from ref. 52 for gamma-quenched U - 10 wt% Mo, Russian data from KONOBEEVSKY (7) for gamma phase of U - 9 wt% Mo alloy annealed 5 hr at 900°C. Accuracy of the values of ref. (7) may be questionable: U - 9 Mo data do not show a behaviour with increasing temperature which is consistent with the behaviour of other uranium alloys: fig. 38.

Post-irradiation physical properties have been published in APDA fuel development programs (38). Compared by the transient heatwave method, irradiation affected the thermal conductivity of U - 10 wt% Mo alloy as follows: no changes in thermal conductivity were observed to burn-ups of

0.35 at %, but a drop of about 15% was observed on specimens irradiated between 0.5 and 1.2 at %.

5.3 Specific heat

The specific heat of U - 10 wt% Mo was estimated by STATHOPLOS (53) using the Kopp-Neuman Law, from the specific heat of gamma uranium and molybdenum. The calculation indicates that from room temperature to 1000°C the specific heat of U - 10 wt% Mo is substantially constant at 0.042 Btu/lb-°F(= cal/g-°C).

Specific heat as a function of the temperature, from M.S. FARKAS and E.L. ELDRIDGE, is reported by ref. (54): Table 5.

5.4 Thermal expansion

An average thermal expansion coefficient of $13.6 \times 10^{-6}/°C$, from 100 to 400°C, is reported by ref. (11) for a U - 10 wt% Mo alloy.

Data from SALLER et al. (22) for U - 9 wt% Mo are reported in Table 6.

KONOBEEVSKY et al. (7) indicate the mean values of the thermal expansion coefficient in the ranges 20 - 300 and 20 - 500°C, for the alloy U - 9 wt% Mo: 12.0×10^{-6} and $12.3 \times 10^{-6}/°C$, respectively. The coefficient varies over the range 20 - 500°C according to the equation

$$\alpha = 11.6 \times 10^{-6} + 0.28 \times 10^{-8}\ T.$$

APDA data from ref. (52) for the instantaneous thermal expansion coefficient are reported in Table 7.

The following coefficients of thermal expansion have been reported by REPAS et al. (20):

for U - 10 wt% Mo alloy:	$18.7 \times 10^{-6}/°C$ in the 500-575°C range
	$22.0 \times 10^{-6}/°C$ in the gamma phase region
for U - 8 wt% Mo alloy:	$18.8 \times 10^{-6}/°C$ in the 500-575°C range
	$20.7 \times 10^{-6}/°C$ in the gamma phase region

The coefficients of thermal expansion at gamma temperatures decrease with increasing molybdenum content, and are larger than the coefficient in the alpha range.

On the post-irradiation linear thermal expansion the following conclusions of LEESER et al. (34) are reported. The effect of irradiation on the U - 10 wt% Mo alloy expansion is summarized in fig. 39. The curve for the expansion of the unirradiated specimen represents an average for a heating and cooling cycle. No significant effect of difference in burn-ups between 0.97 and 2.0 at % on thermal expansion between room temperature and 500°C (932°F) was noted. However, irradiation has apparently produced an increase in the rate of expansion for the alloy when compared with the unirradiated control specimen. Probably of greater significance, however, is the overall length increase resulting from a single cycle to 500°C. In addition to the length increase, density and electrical resistivity measurements showed that the dilation test had produced both a density decrease and a decrease in resistivity, indicative of the initiation of gamma-phase decomposition. Consequently, the change in linear thermal expansion characteristics accompanying irradiation is probably the result of the initiation of transformation and concomitant swelling in the absence of a neutron flux. It should be noted that both of these specimens had been irradiated previously at the maximum temperature of about 600 $\pm$ 90°C (1112°F) with density changes of 3.5 and 3.9% being observed. These changes occurred during a minimum of 58 days of irradiation while density changes of 0.9 and 2.1% accompanied post-irradiation heating and cooling over a 6 hr period.

A dilation curve for a specimen irradiated to 1.4 at % burn-up and tested to 800°C is also shown in fig. 38. A marked increase in rate of expansion occurs above 550°C, indicative of the onset of swelling in the specimen. A density decrease of 3.2% was found to result from this test. The temperature at which swelling occurs during post-irradiation heating cannot be correlated with the temperature at which swelling is observed during in-pile irradiation for this alloy.

5.5 Hardness

The diamond pyramid hardness (DPH) values for U - 10 wt% Mo from ref. (55) are the following:

gamma-quenched from 800°C : 280 DPH
isothermally aged 500°C 8 hr: 310 DPH

A value of about 300 DPH for gamma phase U - 10 wt% Mo alloy is indicated by LEESER (34).

Vickers hardness values indicated by ref. 56 are reported in fig. 40 as a function of the molybdenum content.

Hot hardness values are reported by SALLER (22): Table 8, and by WALDRON et al. (57): Table 9.

In the experimental work of BLEIBERG (35), the hardness of irradiated gamma-quenched uranium-molybdenum alloys increased with exposure to a saturation level above which further burn-up produced no additional hardening. The total increase was 91 DPH units, produced by about 800 MWd/te; values are reported in Table 10.

Hardness measurements obtained by LEESER (34) during the course of post-irradiation metallographic examinations showed that only a slight increase in hardness as a result of irradiation, an increase in hardness for the gamma phase U - 10 wt% Mo alloy, of between 30 to 50 DPH accompanied irradiation to burn-ups of 2.2 at %.

Irradiation influence on the hardness of U - 7% and U - 9% Mo alloys has been reported by DMITRIEV et al. (48). The hardness of the alloys irradiated in the gamma phase was practically not changed; for the alloys irradiated in the $\alpha + \gamma'$ state the hardness decreased: Table 11.

5.6 Tensile tests

The mechanical properties of the uranium-molybdenum alloys vary with mo-

lybdenum content, and above all with the fabrication history and the thermal treatment of the material. Tensile properties have been studied by several laboratories. A stress-strain curve for U - 10 % Mo alloy is shown in fig. 41 (58).
The results of the studies of WALDRON et al. (57) are reported in Table 12.

APDA data reported by ref. 52 (1962) relating to the variation of tensile properties of gamma-quenched and quenched plus aged U - 10 % Mo alloy with test temperature are reported in Table 13.

A summary of some Russian data is reported by GITTUS (1) (1963); the data relating to alloys with molybdenum content of zero - 7.8 - 10 - 10.9 % are indicated in Table 14.
Mechanical properties of U - 10 % Mo alloy, determined by PETERSON and VANDERVOORST (55) (1964) are reported in Table 15.

Tensile tests have also been performed by HILLS, BUTCHER and HOWLETT (59) (1964): the results for U - 9.1 % Mo and U - 10.5 % Mo are reported in Table 16.

Ultimate tensile strength data of the above mentioned references are represented in fig. 42: the data are for 10 ÷ 10.5 Mo alloys, in the gamma-quenched condition. Mechanical properties show an evident and considerable spread of the values; it is impossible to rationalize these differences, which may be attributed to differences in strain rate, material purity, grain size, experimental techniques.

The general behaviour of the alloy is not very ductile. The ductility of the alloys in some investigations was probably affected by non-metallic inclusions (57). By comparing data of different works, HILLS, BUTCHER and HOWLETT (59) suggest that the precipitates due to the impurities must have a large embrittlement effect on the alloys.
It is believed that higher purity alloys are less brittle (60).
Alloys prepared with more recent ameliorated casting techniques are more ductile; a confirmation is given by the data reported by PETERSON and VAN-

DERVOORST (55) : Table 15. The interstitial impurities H, N, O, C are the lowest of all the considered alloys and the elongations are the best.

Generally, uranium-molybdenum alloys have a great susceptibility to stress-cracking.
HILLS, BUTCHER and HOWLETT (59) have studied and discussed two forms of cracking that were found performing tensile tests at room temperature; specimens were mercury- and oil-quenched gamma phase alloys.
A circumferential cracking is due to stress corrosion by air. An intergranular cracking, in the alloys with more than 9% molybdenum, is difficult to explain but it is related to a grain boundary brittleness.
The high susceptibility of U - 10 Mo alloy to cracking when stressed in air was studied by PETERSON and VANDERVOORST (58); oxygen was determined to be the embrittling agent. In these alloys the elongation in a stress-strain test is sensitive to strain rate, and the maximum ductility is obtained at a rate of about 0.05 in/in/min : fig. 43. Delayed failure was observed at a stress as low as 26 kg/mm^2 (30% of the yield stress). The critical stress appears to be dependent on carbon content, but not on grain size.

A material test program was set up at the Lawrence Radiation Laboratory to determine some properties of U - 10% Mo, with particular reference to those properties of interest to the prompt-burst reactor "Super Kukla". An experimental investigation was undertaken to determine the properties of this alloy under dynamic conditions: ref. (61) (62).
The dynamic tensile tests were conducted on extruded material, hot-rolled material, as-cast material having 800 ppm carbon, and as-cast material having 75 ppm carbon. Temperatures were varied from 24 to 315°C, and strain rates from zero to 100 in/in/sec. The results are summarized in fig. 44 ÷ 47. Peak stress at a strain rate of 20 in/in/sec is plotted as a function of temperature in fig. 48.
Among the conclusions drawn are the following:

a) dynamic loading increases tensile strength and lowers ductility of U - 10% Mo in both the as-cast and wrought conditions. High strain rates affect the mechanical properties through two mechanisms. First, as the strain

rate is increased, the effect of stress corrosion is mitigated as a result of the decrease in time the load is applied. The stress corrosion effect predominates at strain rates less than 1 per sec. Further, high strain rates tend to delay the yield phenomenon and increase the tensile strength.

b) hot-rolled material is superior to cast at temperatures around 150°C and above. At lower temperatures it is exceedingly notch sensitive.

c) cast specimens do not display as consistent mechanical properties as wrought specimens. Cast specimens are also less ductile.

d) high carbon content tends to reduce both ductility and tensile strength in cast material. As not yet conclusive observation, it is said that the carbon content should be kept below 200 ppm.

Post-irradiation mechanical properties of the U - 10% Mo alloy were determined on specimens irradiated to burn-ups of 2.1 total at % (34) (63). The effect of burn-up on ultimate strength and strain at fracture for a 500°C test temperature is shown in fig. 49. A marked reduction in strength and ductility is seen to exist after irradiation, with the most drastic reduction occurring prior to burn-up of 1 at %. Clad specimens were observed to exhibit greater ductility than bare specimens, this is believed to result primarily from reduction in effective surface defects. It must be noted that during the course of testing, the specimens were effectively subjected to a post-irradiation heat treatment, with partial decomposition of the gamma phase; this transformation affects the mechanical properties.
Post-irradiation mechanical property data are not believed to be directly applicable to in-pile behaviour when obtained during tests at elevated temperatures, and the interpretation of post-irradiation temperature effects is difficult.

5.7 YOUNG's modulus

The temperature dependence of the YOUNG's modulus of the U - 9% Mo

alloy, from KONOBEEVSKY et al. (7) is shown in fig. 50. The elasticity modulus was determined by the resonance method with specimens subjected to homogenizing annealing in the gamma phase and with specimens annealed below the temperature of the eutectoid transformation. The YOUNG's modulus of the gamma phase of this alloy is much lower than that of pure alpha uranium. After prolonged annealing below the temperature of the eutectoid line, the elasticity modulus of the alloy increases because of the decomposition of the gamma phase, which results in the formation of alpha phase grains.

WALDRON et al.(57) have published a relation between YOUNG's modulus and the temperature, for U - 7.8 Mo, U - 10% Mo, U - 10.9% Mo alloys: Table 17.
Values of YOUNG's modulus for U - 10% Mo alloy, from the APDA data published in ref. 52, are reported in Table 18, as a function of the temperature.
A comparison of the values for the gamma phase alloys as reported by the above mentioned authors, is given in Table 19.

The elastic modulus of irradiated U - 10% Mo specimens was determined by LEESER et al. (34). The effect of temperature on the YOUNG's modulus is shown in fig. 51. YOUNG's modulus is seen to decrease with test temperature and with burn-up. The temperature of irradiation appears to modify the amount of reduction experienced for a given burn-up. Thus, specimens irradiated at higher temperatures to comparable burn-ups show a lesser reduction in modulus. Presumably, the annealing action at higher temperatures reduces radiation-produced changes in the alloy structure.

Consequently to the partial decomposition of the gamma phase which occurs during the course of testing, at the 500°C test temperature in particular, a portion of the change in mechanical properties is undoubtedly obscured by transformation. For this reason, the direct application of properties determined by post-irradiation measurements to in-pile behaviour is not regarded as valid.

5.8 Creep

Creep data for uranium-molybdenum alloys, at 815°C, are given in Table 20 (64).

5.9 Impact strength

Impact properties as determined by McGEARY (11) are reported in Table 21 (unnotched Izod specimens): tests show brittle fracture below 66°C and ductile above.

Charpy V-notch impact values have been determined by PETERSON and VANDERVOORT (55) for U - 10% Mo alloys:

gamma-quenched from 800°C : 7 - 10 ft-lbs
isothermally aged 500°C - 8 hr : 6 - 7 ft-lbs

5.10 Fatigue

A curve of total strain versus cycles to failure has been reported by K.G. HOGE (62), for cast and wrought specimens of U - 10% Mo alloy: fig. 52.

6. ACKNOWLEDGEMENT

Thanks are due to Mr. J.A. LARRIMORE, SORA Project Leader, for helpful discussions and revision of the manuscript.

TABLE 1

Total cumulative vol. -% increases during post-irradiation annealing in U - 10% Mo alloy (ref. 51).

	Alloy			
	A	E	F	G
After irradiation	10.0	1.4	0.5	1.0
72 h at 550°C	42.9	2.4	0.7	1.0
24 h at 600°C	-	1.7	1.2	1.8
24 h at 750°C	-	3.4	0.9	1.8
24 h at 850°C	-	4.6	1.7	3.2
24 h at 950°C	-	8.5	4.2	6.5

Alloy A: Uranium - alpha phase
heat treated 1 day at 600°C, furnace cool

Alloy E: U - 10.3% Mo - gamma phase with 10% eutectoid
heat treated 1 day at 1000°C, water-quenched, 15 days at 550°C air cool

Alloy F: U- 10.5% Mo - 0.04 Sn - gamma phase with trace eutectoid
particle size 0.3×10^{-4} cm - density 2×10^{13} particles/ cm^3
heat treated 53 h at 1100°C, water-quenched, 10 days at 550°C air cool

Alloy G: U - 10.5% Mo - 0.04 Sn - gamma phase with trace eutectoid
as-cast

Irradiation data: calculated central temperature: 400°C
burn-up analysis: 0.59 at %
thermal neutron flux: 1.10^{14} neutrons/cm^2

TABLE 2

Variation of density with molybdenum content of gamma-quenched uranium-molybdenum alloys - ref. 11.

Mo content wt %	Density at 20°C g/cm^3
0	18.7-19.0
2.5	18.3
5	18.0
7.5	17.6
10	17.2
15	16.6
20	16.0
25	15.5

TABLE 3

Variation of density with temperature for gamma-quenched U - 10 wt% Mo alloy - ref. 52.

Temperature °C	Density g/cm^3
25	17.13
100	17.06
200	16.97
300	16.88
400	16.80
500	16.71
550	16.66

TABLE 4

Variation of thermal conductivity with temperature for gamma phase uranium molybdenum alloys.

Temperature °C	Thermal conductivity cal/cm-sec-°C	
	U-9 Mo (ref. 7)	U-10 Mo (ref. 52)
25		0.029
100	0.040	0.034
200	0.050	0.041
300	0.064	0.048
400	0.078	0.055
500	0.092	0.063
600		0.072
700		0.081
800		0.090

TABLE 5

Specific heat of gamma-phase uranium - 10% molybdenum (ref. 54)

Temperature °C	Specific heat cal/g-°C
0	0.0322
100	0.0339
200	0.0357
300	0.0375
400	0.0393
500	0.0410
600	0.0428
700	0.0446
800	0.0463
900	0.0481
1000	0.0499

TABLE 6

Average thermal expansion coefficient for U - 9 wt% Mo alloy - ref. 22.

Temperature °C	1 hr 800°C, water quenched		1 hr 800°C, furnace cooled to 500°C, held 200 hr, furnace cooled	
	heating curve	cooling curve	heating curve	cooling curve
20 - 100	12.88	11.80	9.99	11.86
20 - 200	13.42	12.09	11.49	12.57
20 - 300	14.11	12.86	12.63	13.00
20 - 400	14.68	13.61	13.36	13.56
20 - 500	15.22	14.08	14.05	14.08
20 - 600	15.74	14.52		14.57
20 - 700	16.07	15.04	16.92	15.09
20 - 800	16.27	15.71	17.13	15.62
20 - 900	16.39	16.40	17.44	16.26
20 - 950	16.36	16.74	17.51	16.51

TABLE 7

Instantaneous thermal expansion coefficient for gamma quenched U - 10 wt% Mo alloy - ref. 52.

Temperature °C	x 10^{-6}/°C	
	long.	trans. (*)
25	11.5	11.9
100	12.2	13.1
200	13.2	14.5
300	14.2	16.0
400	15.2	17.5
500	16.2	19.0
550	16.6	19.8
600	16.6	19.8
700	17.9	20.7
800	19.2	21.8
900	20.5	

(*) Estimated spread $\pm$ 1.5 x 10^{-6}/°C

TABLE 8

Hot hardness of U - 9% Mo alloy - ref. 22.

Temperature °C	DPH (kg/mm^2)	
	heat treatment A	heat treatment B
room T	276	423
600	86	86.9 [1]
650	69	78.3 [1]
680	-	65.3 [1]
700	51	58.2 [1]
725	-	48.3 [1]
750	38	41.1 [1]
800	30	27.7 [1]

A : 1 hr 800°C, water quenched

B : 1 hr 800°C, furnace cooled to 500°C, held 200 hr, furnace cooled

[1] : transformations may have occurred.

TABLE 9

Hot hardness for U - Mo alloy - ref. 57.

Test temperature °C	Vickers hardness Treatments before water quenching			
	900°C - 7 days			900°C-7 days 450°C-14 "
	7.8% Mo	10.0% Mo	10.9% Mo	10.0% Mo
20	297	316	348	541
100	266	277	254	446
200	166	237	245	216
300	122	200	147	138
400	124	183	130	74.2
500	113	132	117	
600	73.6	128	99.8	
700	27.7	78.5	81.6	
800	29.2	50	44.3	

TABLE 10

Microhardness of irradiated gamma quenched U - 10.5 % Mo samples (extruded material) - ref. 35.

Exposure MWd/T	DPH at 5 kg Load	
	post-irradiation	increase
115	299 ± 3	24 ± 8
375	323 ± 8	48 ± 13
445	283 ± 9	10 ± 14
700	305 ± 4	31 ± 9
900	310 ± 7	35 ± 12
940	317 ± 4	42 ± 9
1050	318 ± 5	43 ± 10
1600	315 ± 2	40 ± 7
2800	329 ± 2	54 ± 7
3000	330 ± 4	55 ± 9
5350	355 ± 3	80 ± 8
5500	369 ± 4	94 ± 9
8500	360 ± 5	85 ± 10
8800	366 ± 2	91 ± 7

TABLE 11

Vickers Hardness of Uranium-Molybdenum alloys - ref. 48.

Mo content wt %	thermal treatment	kg/mm^2	
		Before irrad.	After irrad. ⋆
7.00	3 days 950°C	266	254
7.00	3 days 950°C and 6 days 500°C	417	360
8.95	3 days 950°C	276	277
8.95	3 days 950°C and 6 days 500°C	432	371

⋆ Irradiation data : temperature 100 ÷ 200°C, thermal neutron density $1 \div 2 \times 10^{13}$ n/cm^2, integral flux $0.5 \div 1 \times 10^{20}$ n/cm^2

TABLE 12

Mechanical properties for U - Mo alloys - ref. 57.

Mo content wt%	State of alloy	UTS (kg/mm^2) over elongation (%) Test temperature (^oC)				
		20	200	400	600	800
6.6	G	89.1 / 8.2	67.2 / 4	68.4 / 3		1.7 / 94
	A	103.6 / 0.6	74 / 1			
7.8	G	74 / 1.2	60.4 / 6	56 / 9	39.3 / 5	6.4 / 69
10.0	G	70.4 / 0.1	58.5 / 0.5	41.1 / 1	20.3 / 0	6.4 / 30
	A	33.5 / 0.8	34.6 / 0	29.3 / 0.5		
10.9	G	70.1 / 1.4		34.1 / 0.5	14.8 / 0.5	10.4 / 6

G = 900°C - 7 days before water quenching

A = 450°C - 14 days before water quenching

TABLE 13

Variation of tensile properties of gamma quenched and quenched plus aged U - 10% Mo alloy with test temperature - ref. 52.

Test temp. °C	Yield strength kg/mm^2		Tensile strength kg/mm^2		Elongation %	
	γ Q	aged	γ Q	aged	γ Q	aged
27	95.6		101.2	111.1	8.8	~1
93	86.5		90.7	106.9	8.7	~1
204	75.2	93.5	76.6	98.4	8.4	1.4
316	64.7	75.9	63.3	89.3	6.0	1.8
427	54.1	59.1	53.4	76.6	2.4	3.0
538	43.6	36.6	46.4	53.4	2.2	6.0
593	38.0	16.9	44.3	28.1	2.3	9.3

γ Q = gamma quenched from 800°C

aged= gamma quenched plus aged two weeks at 500°C

TABLE 14

The relationship between the mechanical properties of U - Mo alloys and temperature - ref. 1.

Test temp. °C	UTS (kg/mm^2) over relative elongation % Mo content (wt %)			
	None	7.8	10.0	10.9
200	31.3 / 24.0	59.5 / 6.0	59.0 / 0.5	-
400	10.8 / 28.0	55.0 / 9.0	40.5 / 1.0	39.5 / 0.5
600	5.7 / 42.1	38.8 / 5.0	19.8 / -	14.5 / 0.5
700	9.0 / 13.0	-	-	16.4 / 1.0
800	-	6.4 / 69.0	6.4 / 30.0	10.2 / 6.0

State of alloy: cast uranium specimens obtained by rolling with subsequent quenching from 900°C in water holding for 7 days at 900°C.

TABLE 15

Tensile properties of U -10% Mo alloys - ref. 55.

State of alloy	Test temp. °C	Strain rate in/in/min	Yield strength kg/mm^2	UTS kg/mm^2	Elongation %
GQ	room T	0.05	85.8	89.3	16.0
GQ	600°C	0.001		33.0	11
		0.01		38.7	3.5
		0.10		40.8	11
GQ	800°C	0.001		11.2	53
		0.01		21.1	39
		0.10		23.2	37
HT	room T		86.5	89.3	. 15

GQ = gamma annealed at 800°C for 1 hour and water quenched

HT = isothermal heat treatment for 8 hours at 500°C.

TABLE 16

Tensile properties at room temperature of uranium-molybdenum alloys - ref. 59.

Mo content wt%	State of alloy	0.1% proof stress kg/mm^2	UTS kg/mm^2	Elongation %
7.9	gamma phase (1)	97.2	103.9	6.0
7.9	gamma phase (2)	89.8	101.6	5.0
9.1	gamma phase (2)	88.2	90.1	9.0
10.5	gamma phase (1)	112.6	112.6	11.5
10.5	gamma phase (2)	113.4	114.6	8.0
11.8	gamma phase (2)	123.8	123.8	7.0

(1) = 950°C for 30 min, mercury quenched
(2) = 950°C for 30 min, oil quenched

TABLE 17

Variation of Elastic Modulus of uranium-molybdenum alloys with tempera- ref. 57.

Mo content wt%	Treatment	Elastic Modulus x 10^3 kg/mm^2				
		20	200	400	600	800
7.8	GQ	8.0	8.0	7.2	7.7	3.8
	AQ	13.3				
10.0	GQ	8.9	7.5	5.3	3.4	4.2
	AQ	12.2	9.3	11.1		
10.9	GQ	9.6	7.7		6.2	5.2

GQ = 900°C - 7 days, water quenched
AQ = 900°C - 7 days, water quenched, 450°C - 14 days, water quenched

TABLE 18

Variation of elastic modulus of U - 10 wt% Mo alloy with test temperature - ref. 52.

Test Temperature °C	Elastic Modulus 10^3 kg/mm^2	
	GQ	aged
27	10.0	12.8
93	9.4	12.2
204	8.7	10.8
316	8.1	9.4
427	7.4	8.1
539	6.7	5.8
593	6.4	3.0

GQ = gamma quenched from 800°C
aged = gamma quenched plus aged two weeks at 500°C.

TABLE 19

Variation of elastic modulus of gamma-phase uranium-molybdenum alloy with temperature.

Test temp. °C	Elastic modulus x 10^3 kg/mm^2			
	9% Mo ref. 7	10% Mo ref. 52	10% Mo ref. 56	10.9% Mo ref. 56
room T	8.6	10.0	8.9	9.6
200	8.1	8.7	7.5	7.7
400	7.7	7.4	5.3	
600	7.1	6.4	3.4	6.2

TABLE 20

Creep data for U - Mo alloys, at 815°C in vacuum; stress 0.35 kg/mm^2 - ref. 64.

Composition $\frac{\text{wt\% Mo}}{\text{wt\% C}}$ and material condition	Time for 1% deformation hr	Minimum creep rate % hr	Test time hr	Total elongation %
7.5/0.13 A	7	0.034	160	4.5
7.8/0.13 A	2	0.052	166	7.5
12.3/0.24 B	29	0.014	172	3.6
13.3/0.27 B	150	0.0023	191	1.1

A = induction melted and cast in graphite, rolled at 900°C
B = induction melted and cast in graphite, canned and rolled at 1200°C

TABLE 21

Impact properties of unnotched Izod specimens of a U - 12% Mo alloy - ref. 11.

Condition	Test temp. °C	Absorbed energy ft - lb	Fracture
as extruded	25	5.7	brittle
GQ	25	2.0	brittle
GQ	66	2.6	brittle
GQ	66	8.9	ductile
GQ	71	14.5	ductile

GQ = 900°C for 24 hr - water quenched.

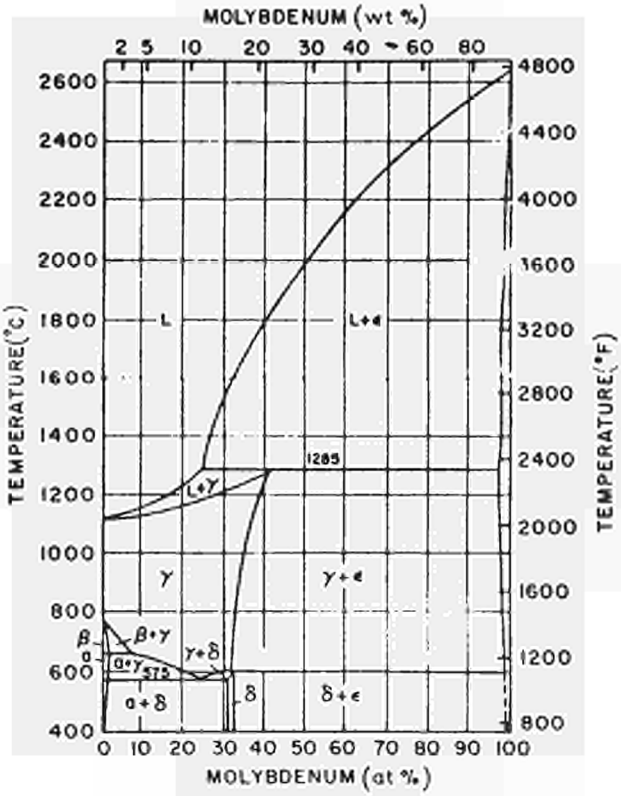

Fig. 1 - Uranium-molybdenum equilibrium diagram from F.A. ROUGH and A.A. BAUER (ref. 3).

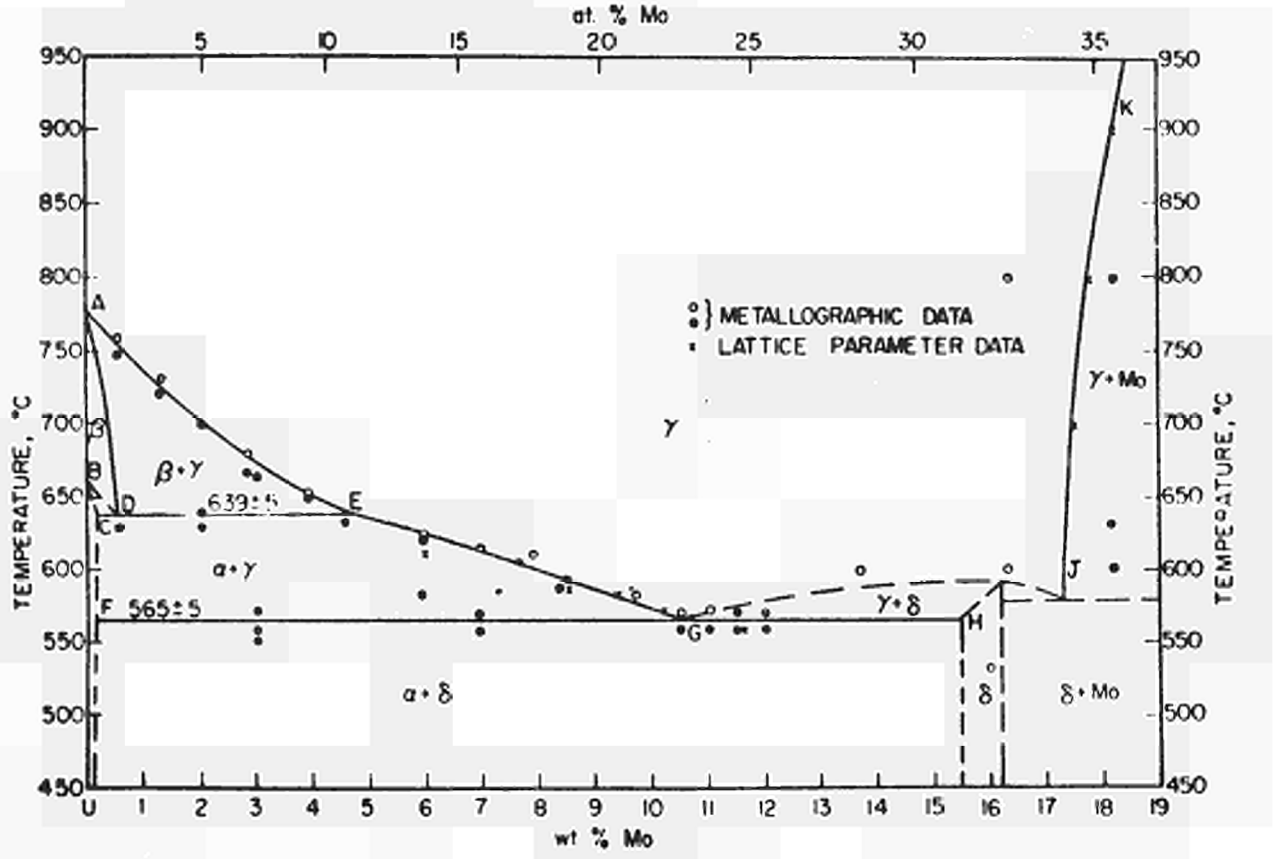

Fig. 2 - Uranium-molybdenum equilibrium diagram to 19 wt% Mo, below 900°C from A.E. DWIGHT (ref. 4).

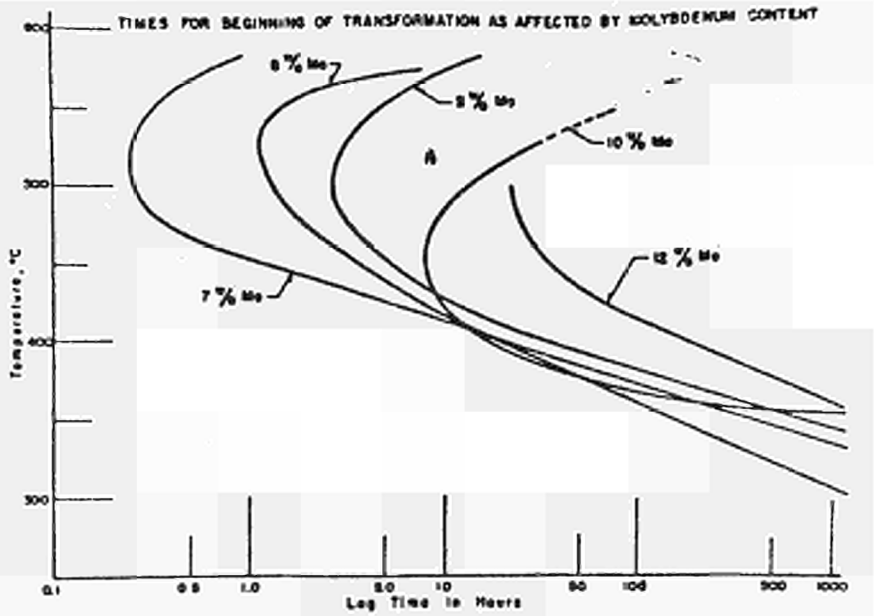

Fig. 3 - TTT diagrams for U-Mo alloys: times for beginning of transformation as affected by molybdenum content from McGEARY (ref. 11).

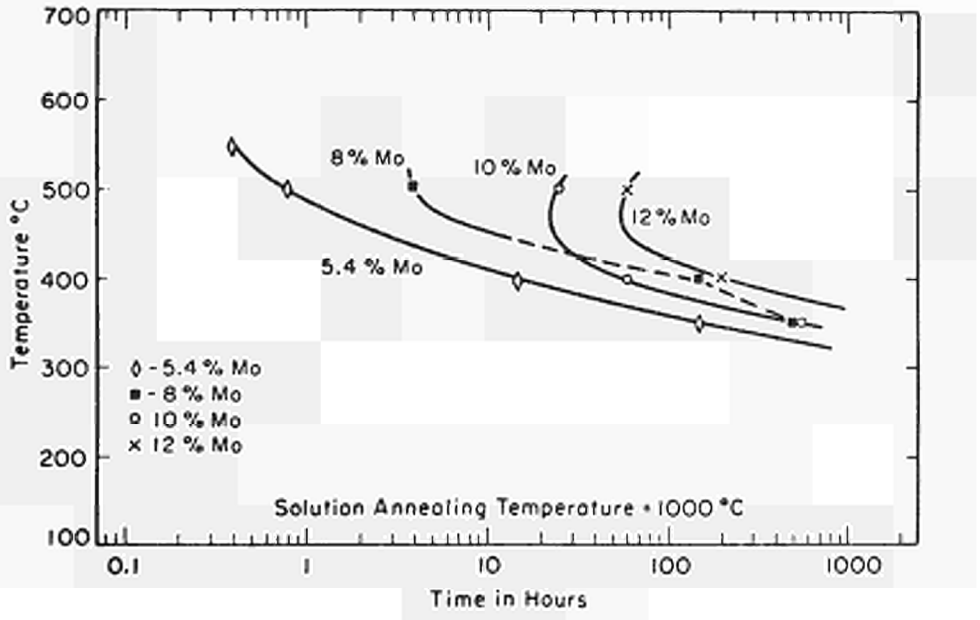

Fig. 4 - TTT diagrams illustrating initial resistivity decrease for U-Mo alloys, from R. J. VAN THYNE and D. J. McPHERSON (ref. 12).

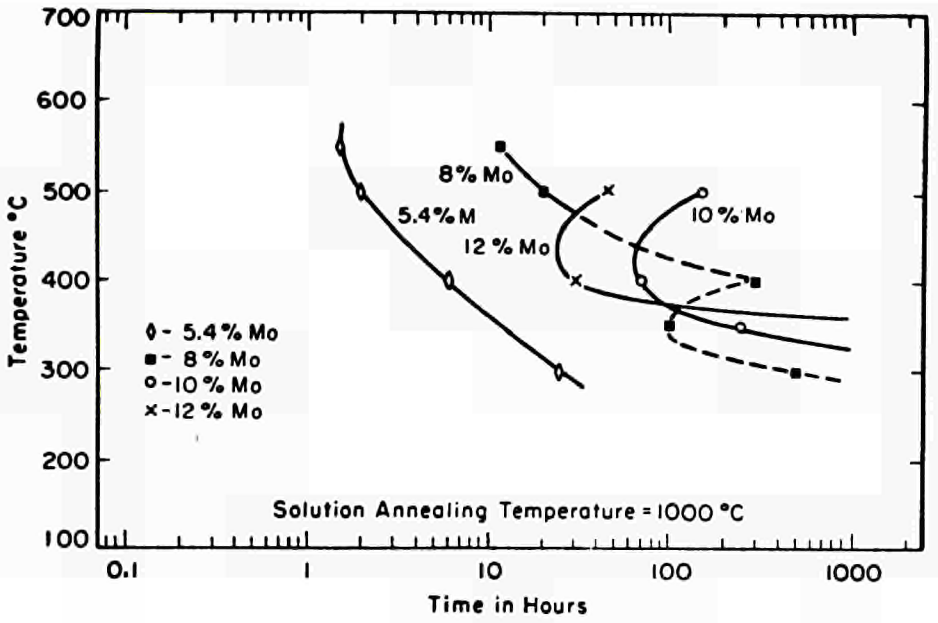

Fig. 5 - TTT diagrams illustrating initial hardness change for U-Mo alloys, from R. J. VAN THYNE and D. J. McPHERSON (ref. 12).

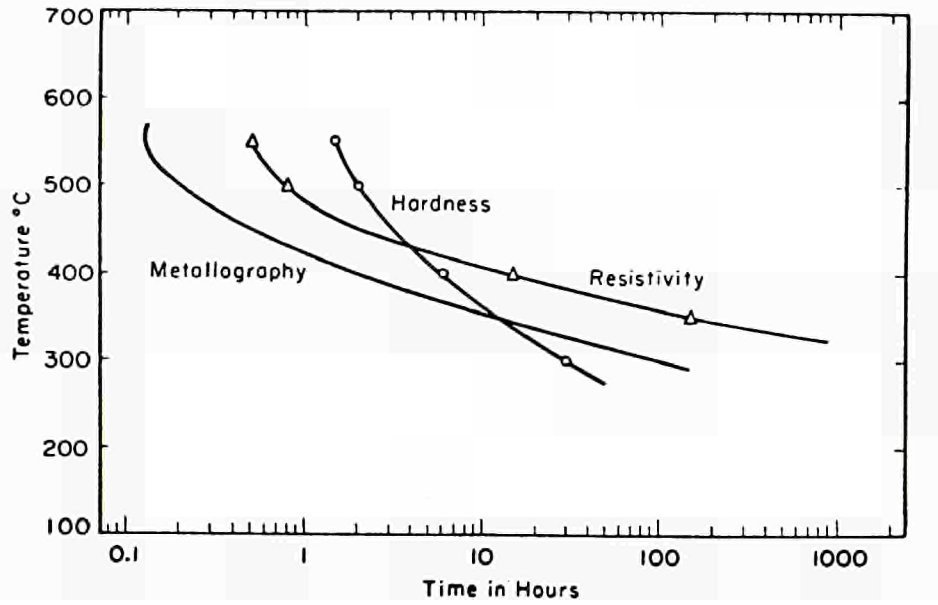

Fig. 6 - TTT diagram for a U-5.4 wt% Mo alloy illustrating initiation of transformation as determined by various techniques, from R. J. VAN THYNE and D. J. McPHERSON (ref. 12).

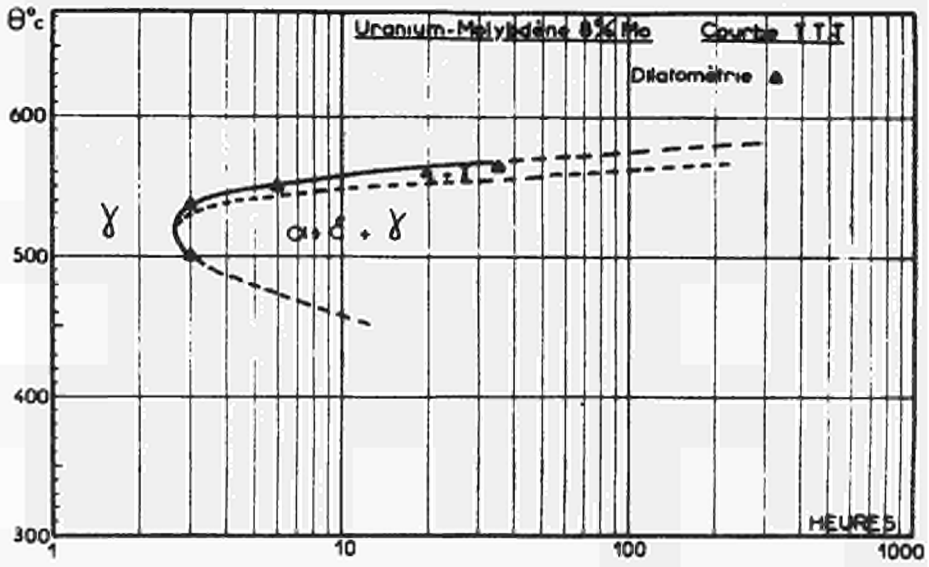

Fig. 7 - TTT diagram for a U-8 wt% Mo alloy as determined by dilatometry, from J. BELLOT et al. (ref. 13).

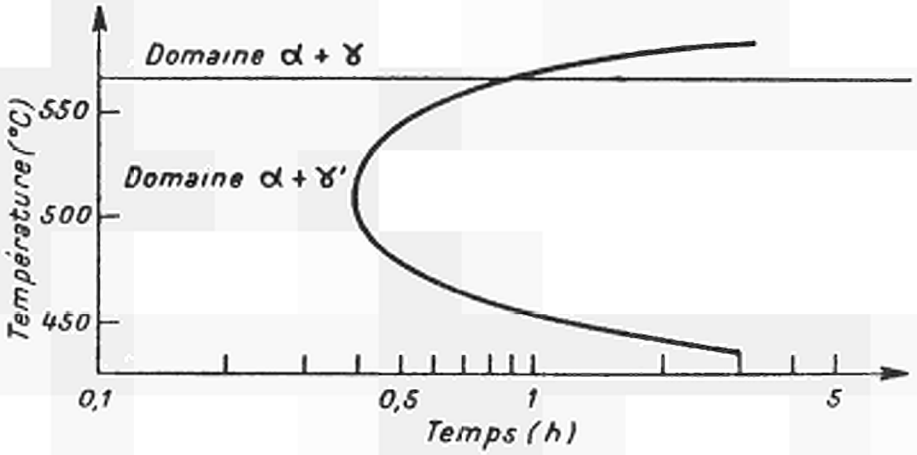

Fig. 8 - TTT diagram for the beginning of transformation in U-8% Mo alloy, from G. DONZE and G. CABANE (ref. 14).

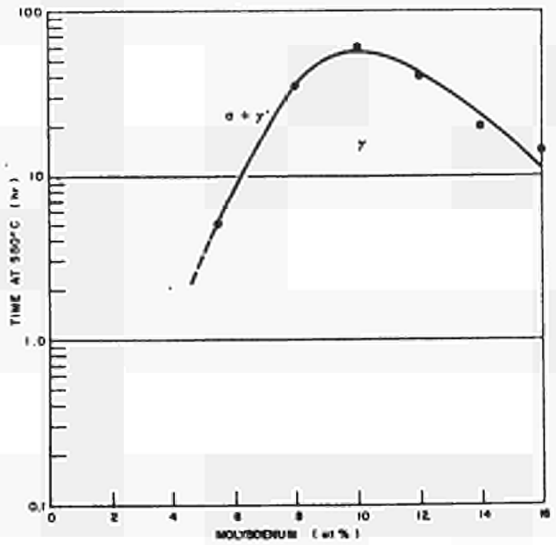

Fig. 9

Variation of time at temperature (550°C) to commence transformation for various molybdenum contents in U-Mo alloys (as determined by X-ray diffraction techniques), from W.A. HOLLAND (ref. 16).

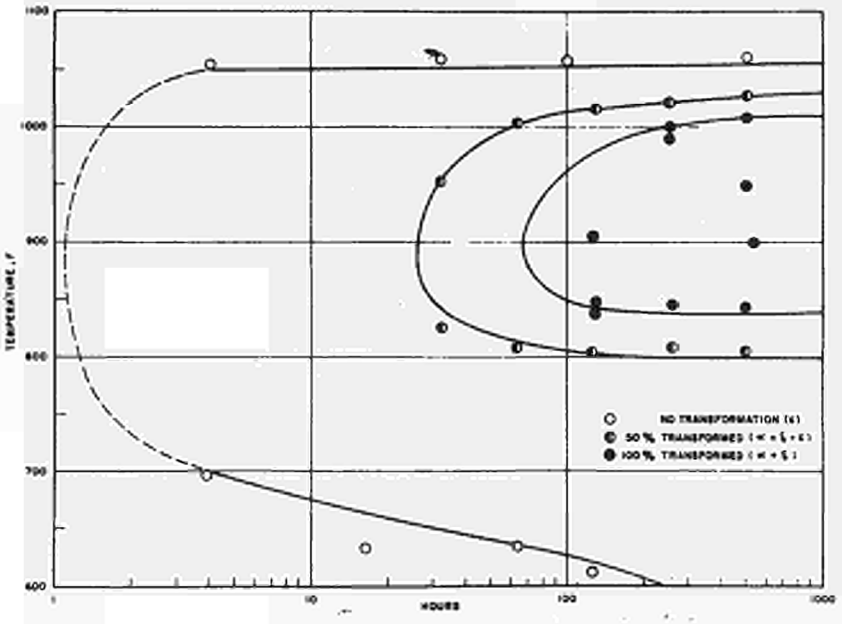

Fig. 10 - TTT diagram for U-10 wt% Mo alloy as determined metallographically, from A.A. SHOUDY et al.(ref. 17).

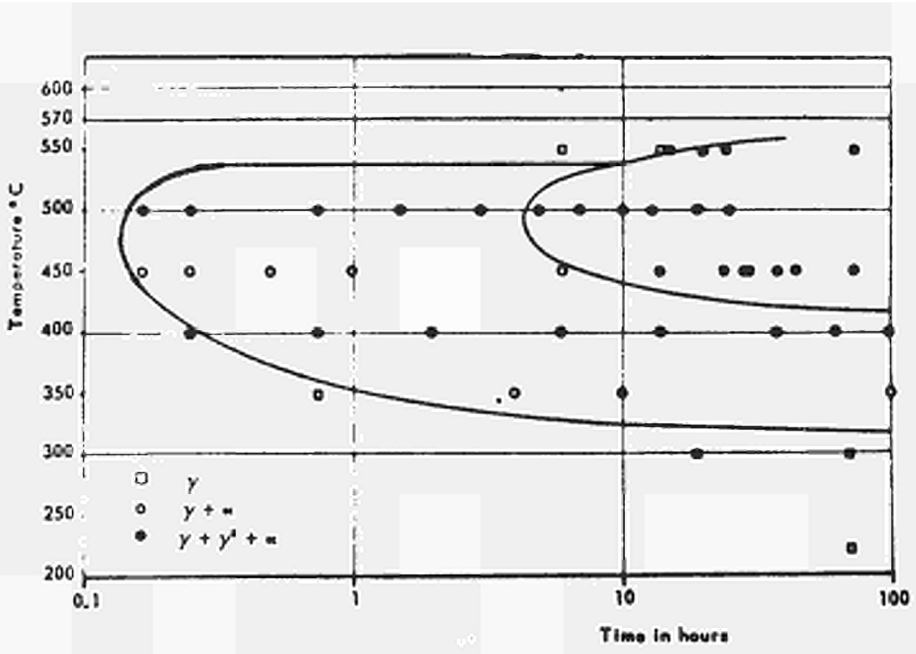

Fig. 11 - TTT curves for U - 10.8 wt% Mo alloy, from A. BAR-OR et al. (ref. 19).

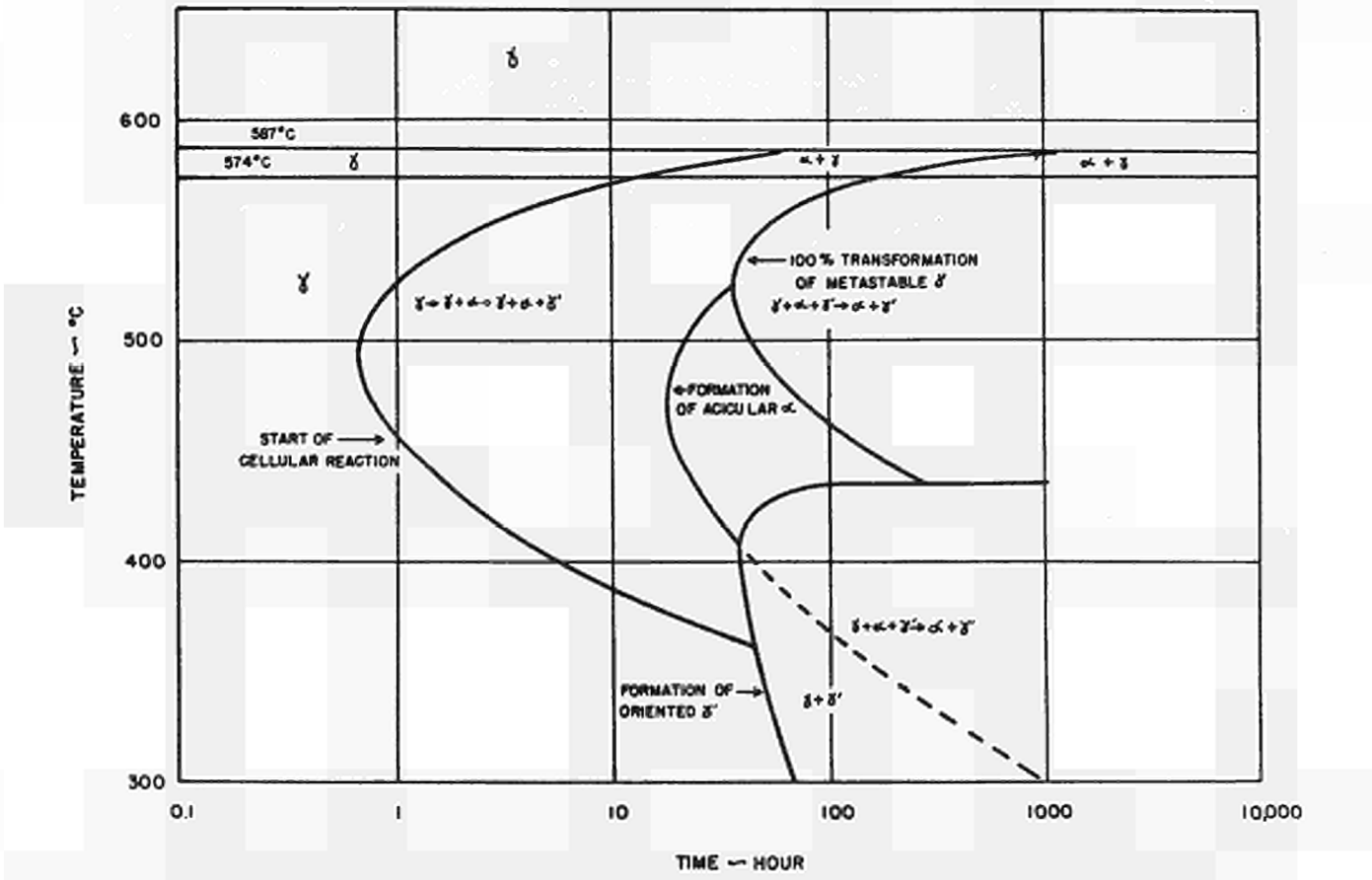

Fig. 12 - TTT diagram for the U-8 wt% Mo alloy quenched to temperature from 900°C, from P.E. REPAS et al. (ref. 20).

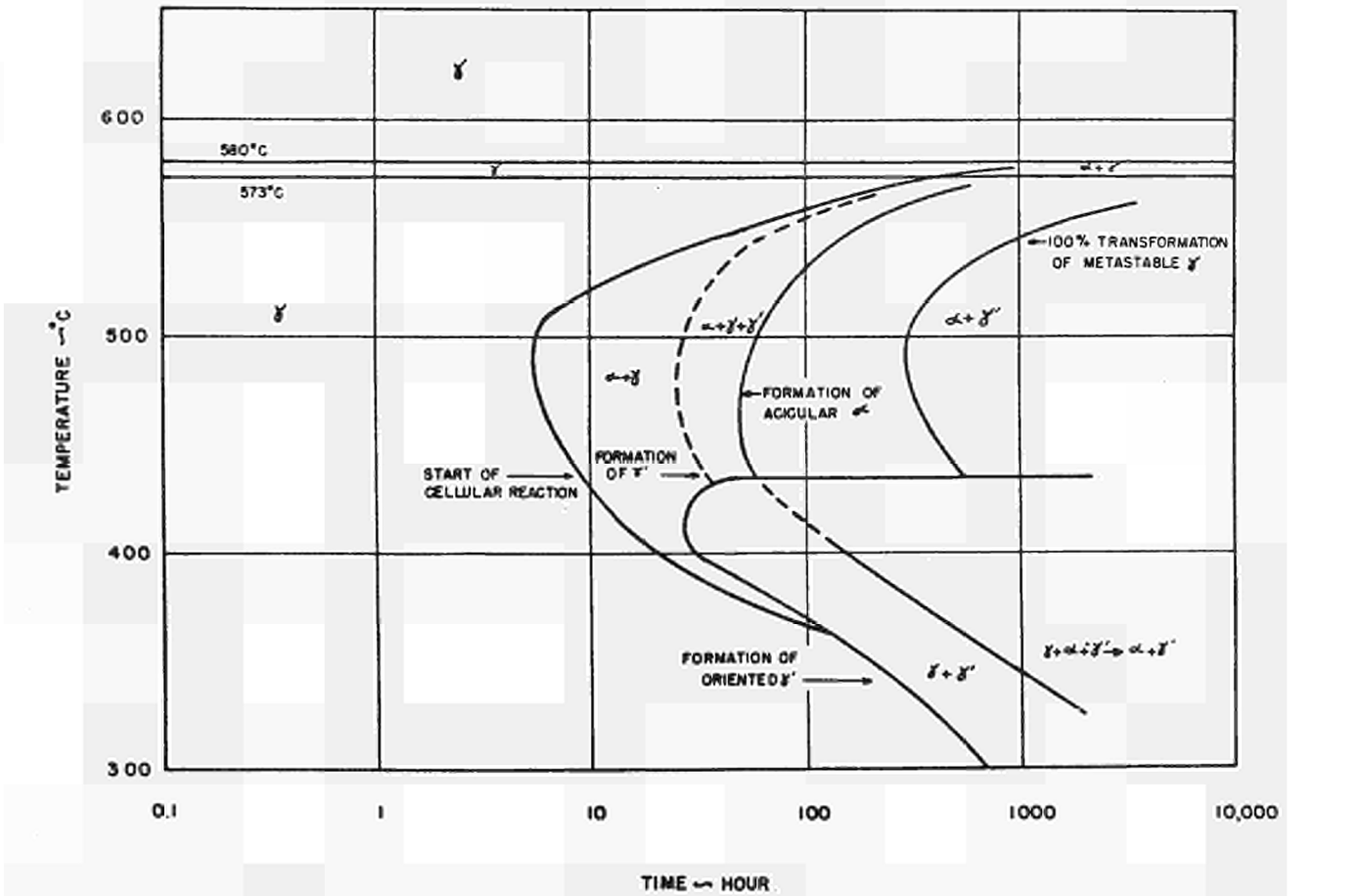

Fig. 13 - TTT diagram for the U-10 wt% Mo alloy quenched to temperature from 900°C, from P.E. REPAS et al. (ref. 20).

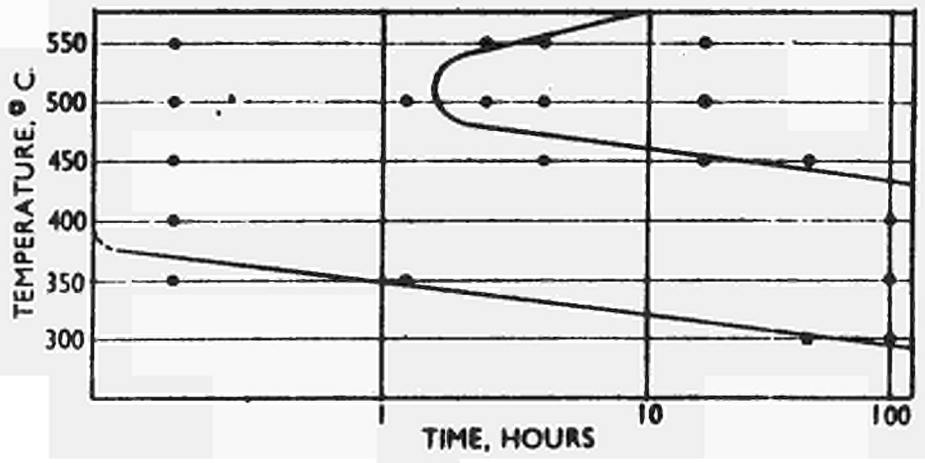

a)

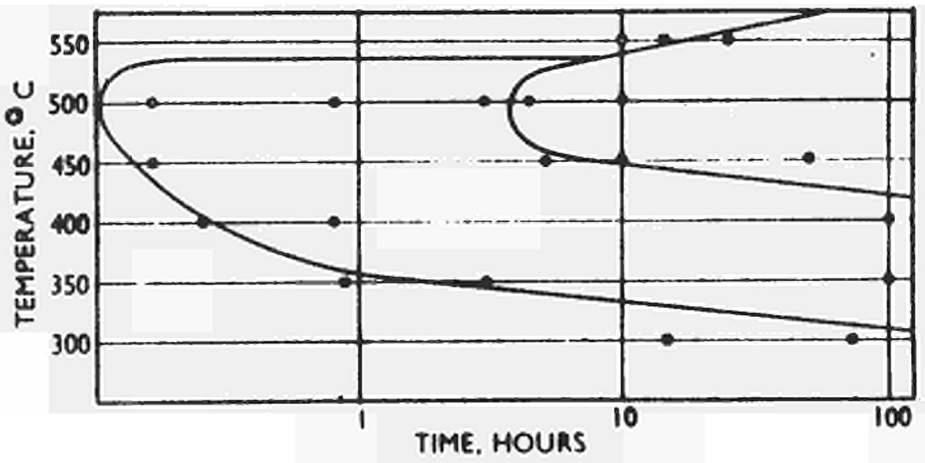

b)

Fig. 14 - TTT curves determined by X-ray powder photography for a) U - 8% Mo alloy; b) U - 10.8% Mo alloy, from Y. GOLDSTEIN and A. BAR-OR (ref. 21).

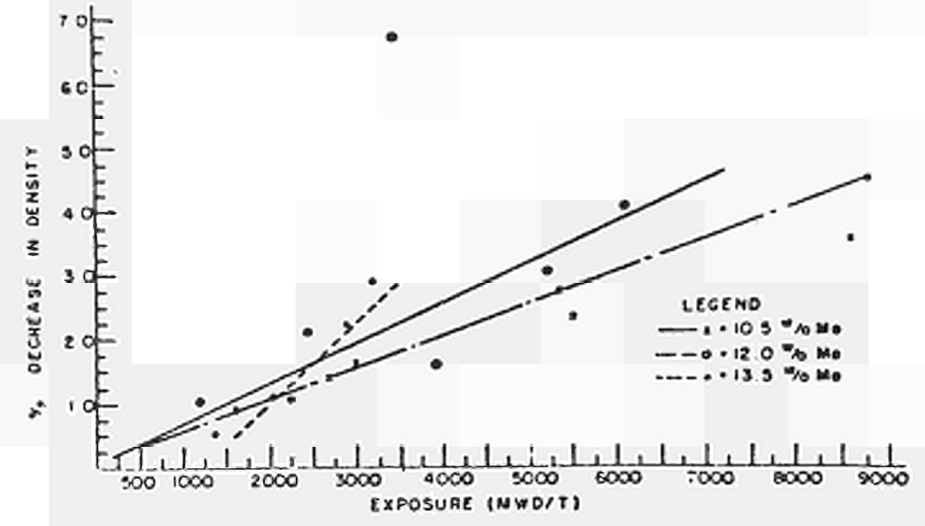

Fig. 15 - Decrease in density versus exposure of irradiated gamma quenched U-Mo alloys, from BLEIBERG et al. (ref. 35).

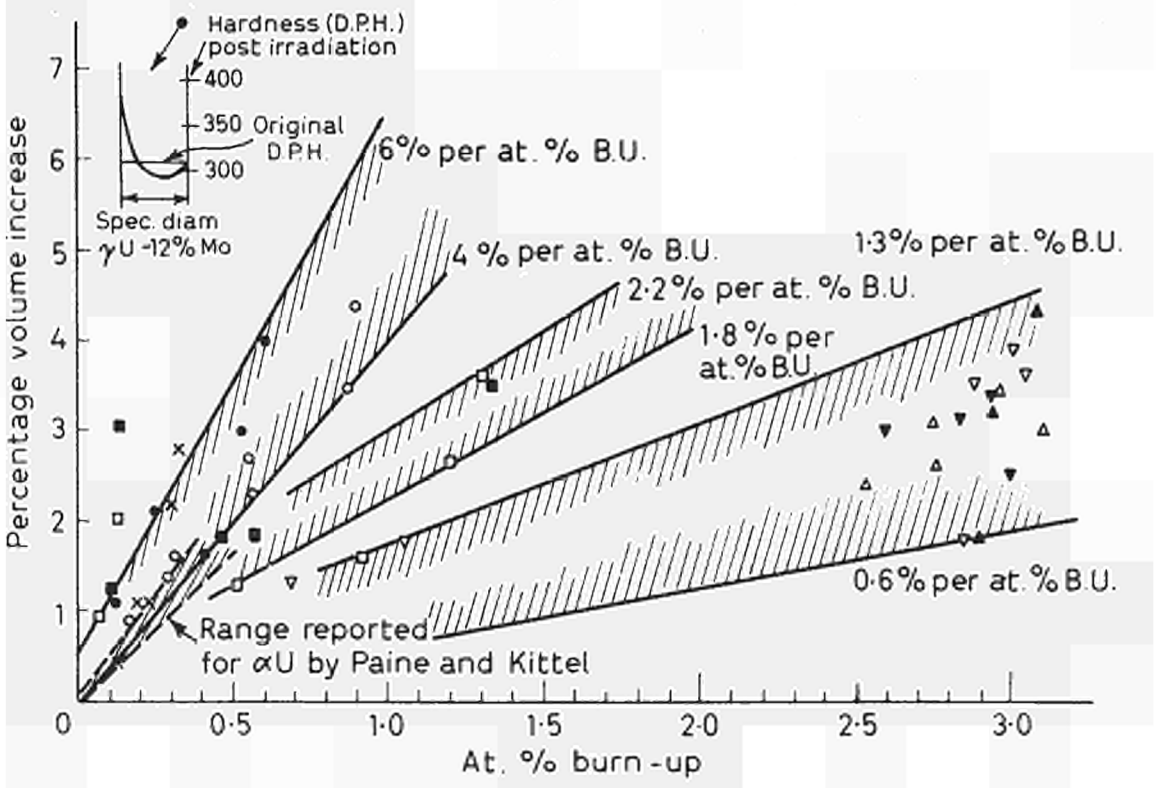

Fig. 16 - Volume changes as a result of irradiation, from BLEIBERG et al. (ref. 35).

o	γU + 10.5 wt% Mo	unclad rods
•	γU + 12 wt% Mo	
x	γU + 13.5 wt% Mo	
□	αU + 2 wt% Zr	0.265" rods clad with 0.02" Zr-2
■	αU	
Δ	γU + 9 wt% Mo	0.244" rods clad with 0.03" Zr-2
▲	γU + 10.5 wt% Mo	
∇	γU + 12 wt% Mo	
▼	γU + 13.5 wt% Mo	

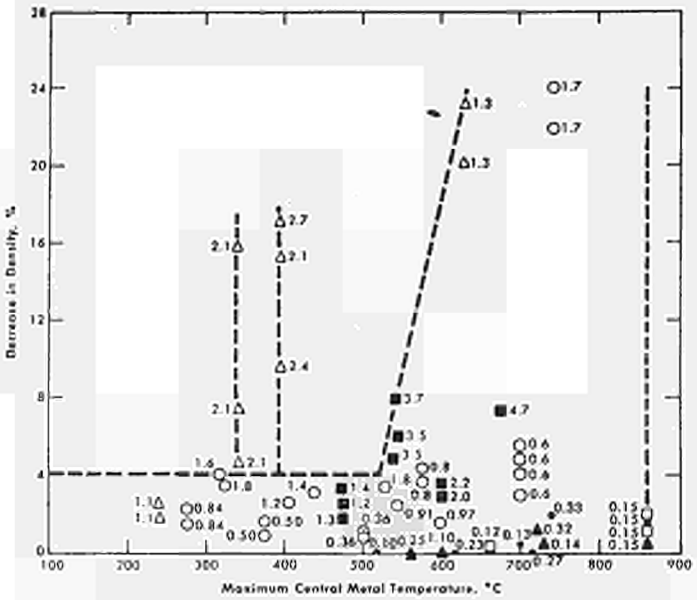

Fig. 17 - Measured decrease in density of U-10 wt% Mo as a function of irradiation temperature (ref. 25).

Values opposite points represent burn-up in at %.

- o hot rolled, unclad; APDA
- ■ coextruded, unclad; APDA
- Δ coextruded, clad; APDA
- ● as cast; AI
- ▲ gamma; AI
- □ transformed (alpha plus epsilon); AI

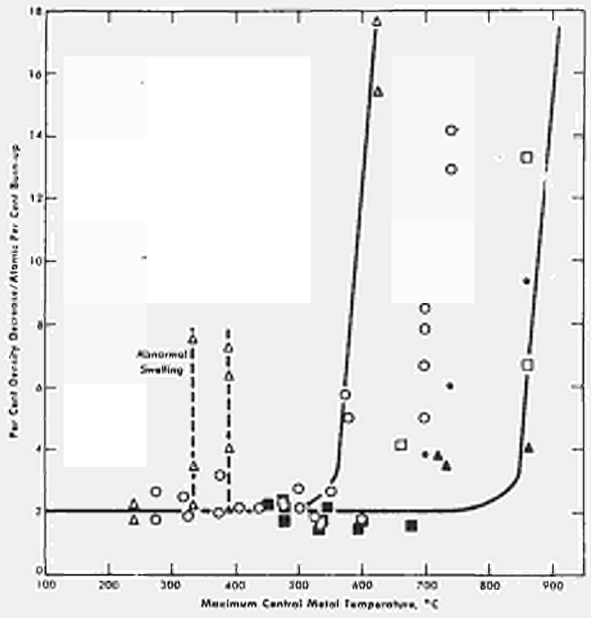

Fig. 18 - Swelling of U-10 wt% Mo as a function of total burn-up (ref. 26).

- o hot rolled; unclad; APDA
- ■ coextruded, unclad; APDA
- Δ coextruded, clad; APDA
- ● as cast; AI
- ▲ gamma; AI
- □ transformed (alpha plus epsilon); AI

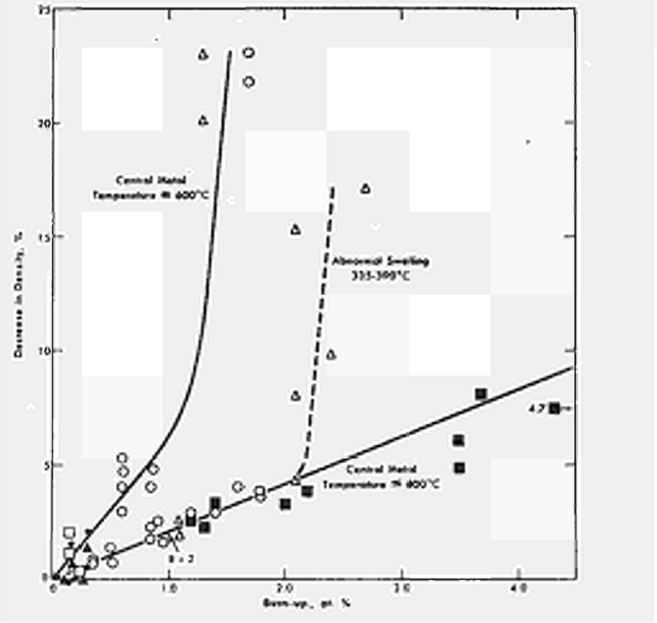

Fig. 19 - Measured decrease in density of U - 10 wt% Mo as a function of total burn-up (ref. 26).

- o hot rolled, unclad; APDA
- ■ coextruded, unclad; APDA
- △ coextruded, clad; APDA
- ● as cast; AI
- ▲ gamma; AI
- ▢ transformed (alpha plus epsilon); AI

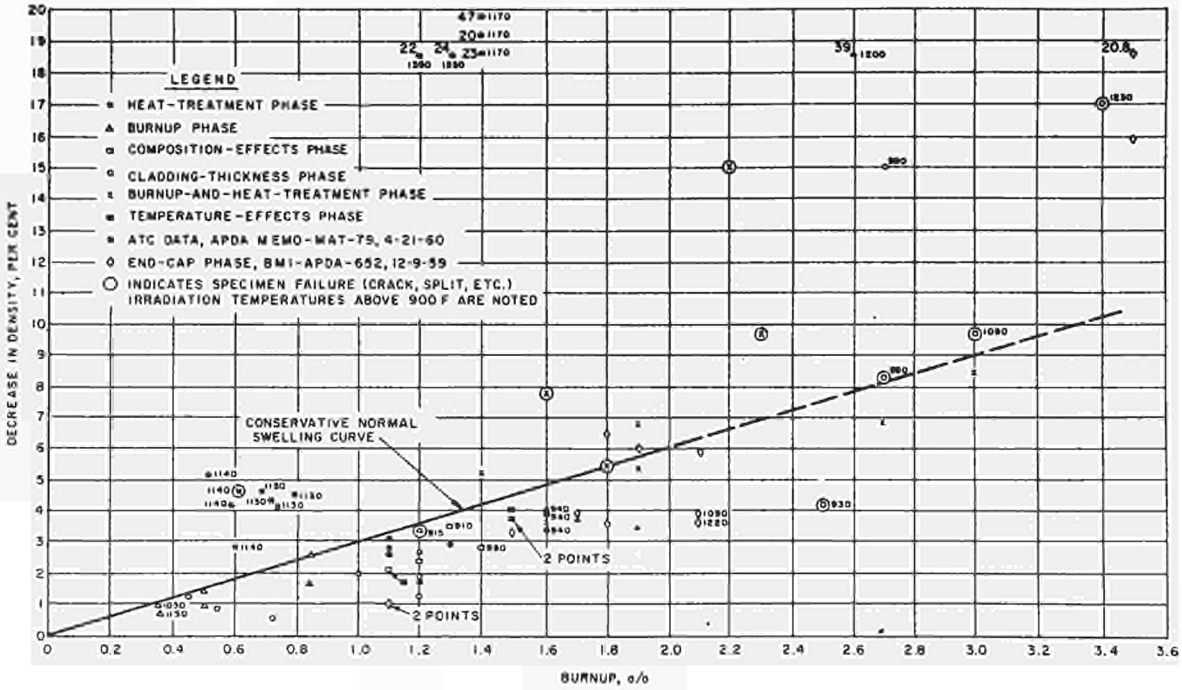

Fig. 20 - Decrease in density of U - 10 wt% Mo alloy specimens as a function of burn-up, from APDA data.

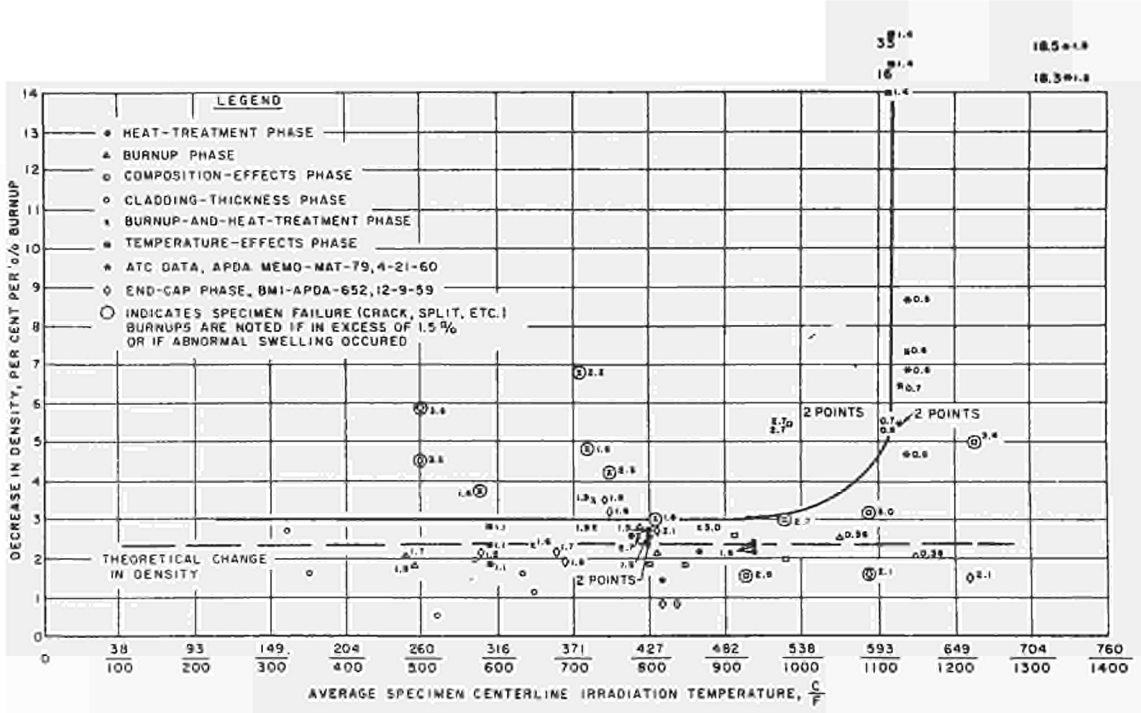

Fig. 21 - Decrease in density of U - 10 wt% Mo alloy specimens normalized to 1.0 at % burn-up as a function of average centerline irradiation temperature, from APDA data.

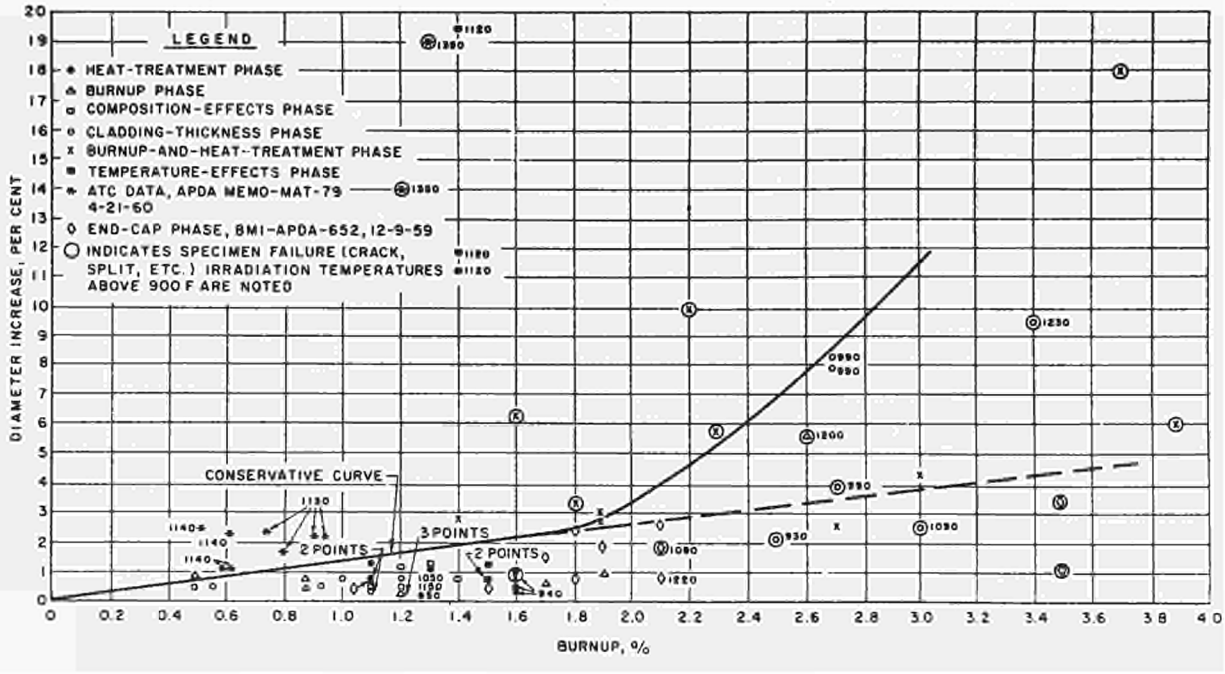

Fig. 22 - Increase in diameter of U - 10 wt% Mo alloy specimens as a function of burn-up, from APDA data.

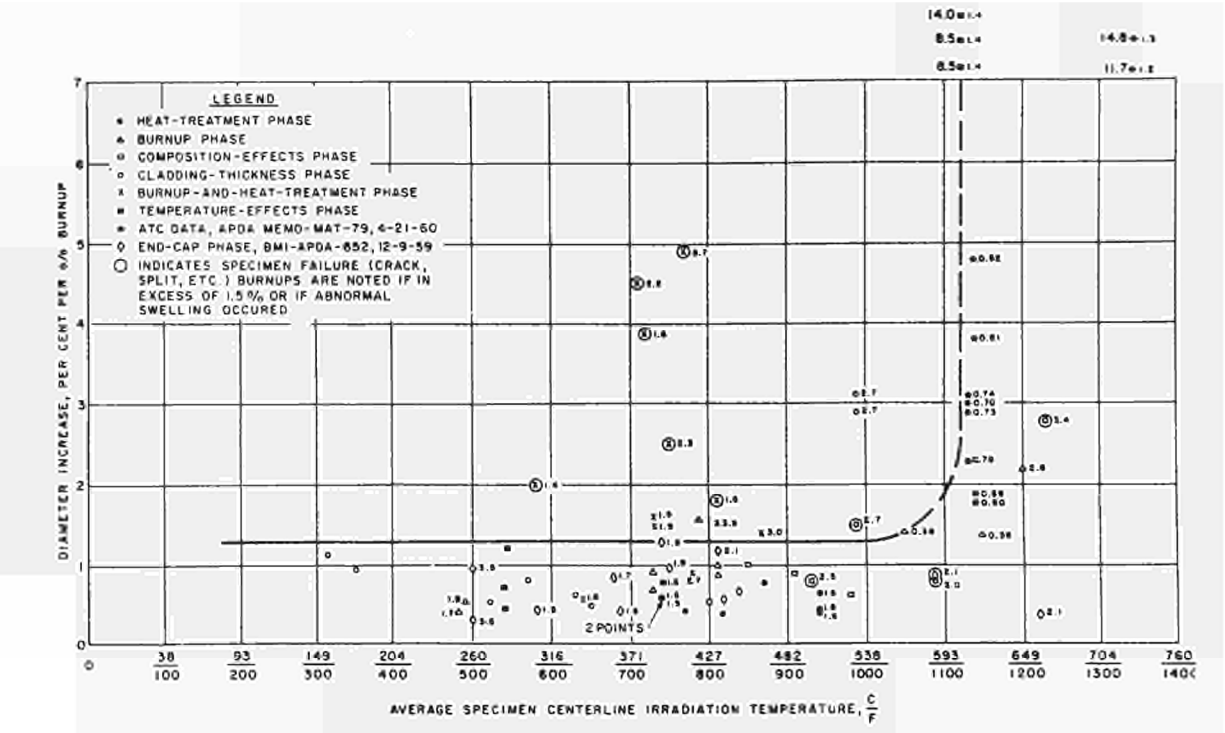

Fig. 23 - Increase in diameter of U - 10 wt% Mo alloy specimens normalized to 1.0 at% burn-up as a function of average centerline irradiation temperature, from APDA data.

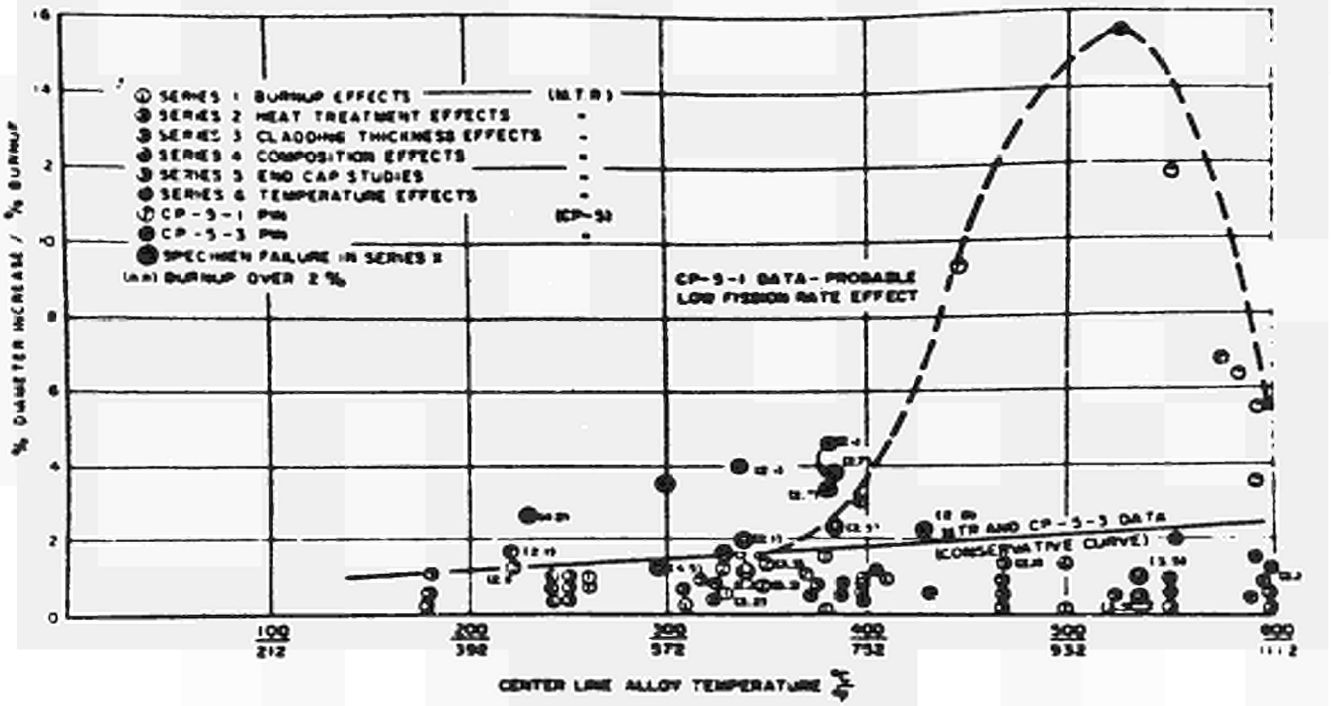

Fig. 24 - Percent diameter increase normalized to 1% burn-up for specimens irradiated at centerline temperature less than 600°C, from BLESSING et al. (ref. 38).

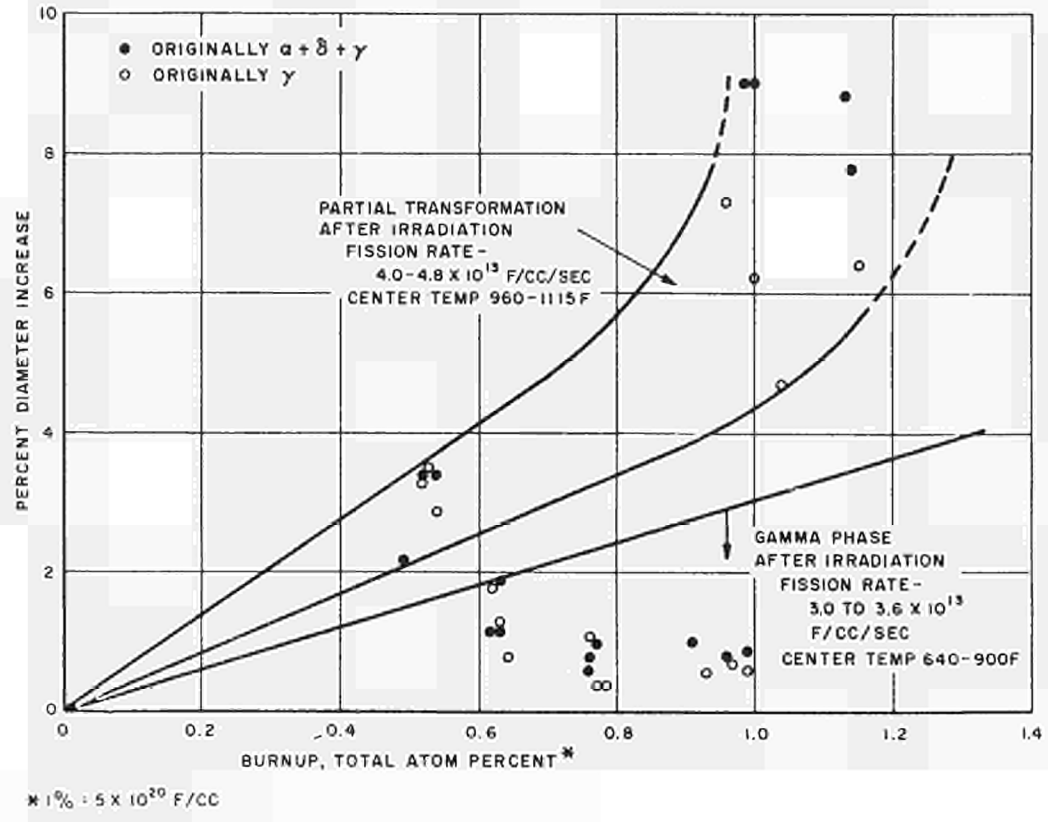

Fig. 25 - Diameter changes versus burn-up for two fission rates and temperature ranges of MTR specimens, from SHOUDY et al. (ref. 17).

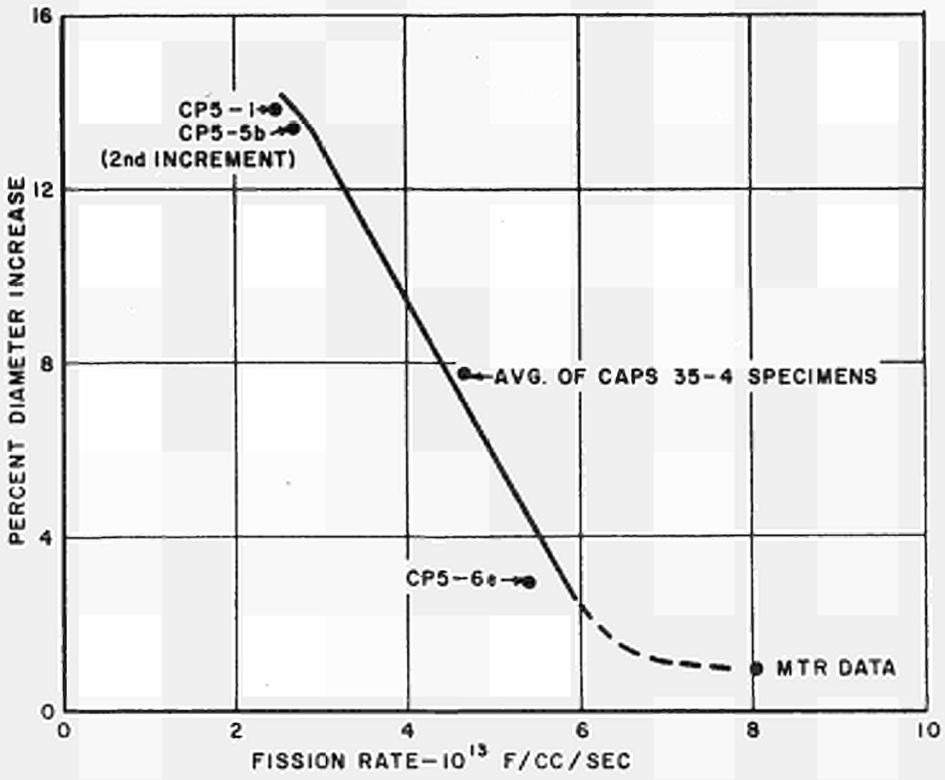

Fig. 26 - Diameter changes versus fission rate for U - 10 wt% Mo specimens irradiated at ~ 520°C to burn-ups of 1.0 ± 0.15 at %, from SHOUDY et al. (ref. 17).

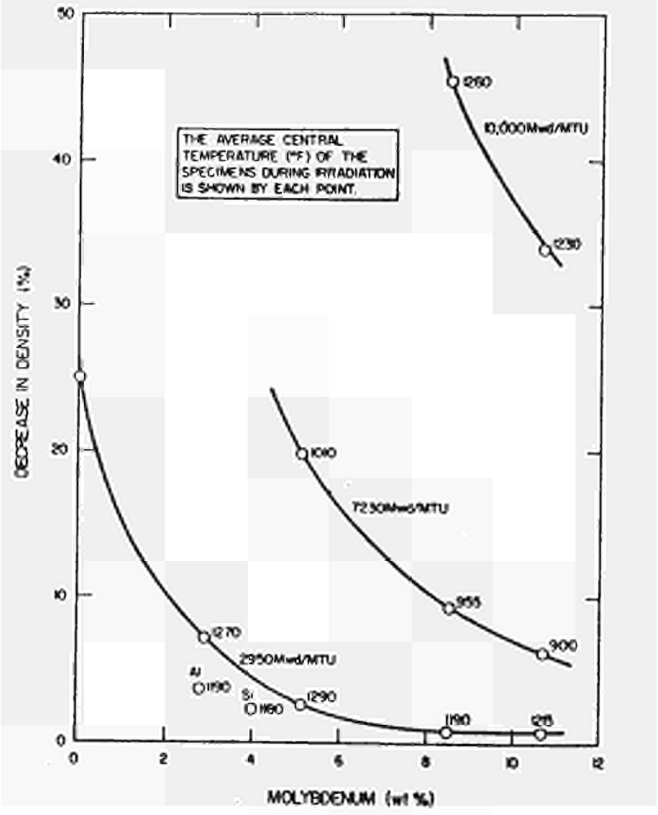

Fig. 27 - Effect of Molybdenum content on swelling of Uranium alloy from JOHNSON and HOLLAND (ref. 40).

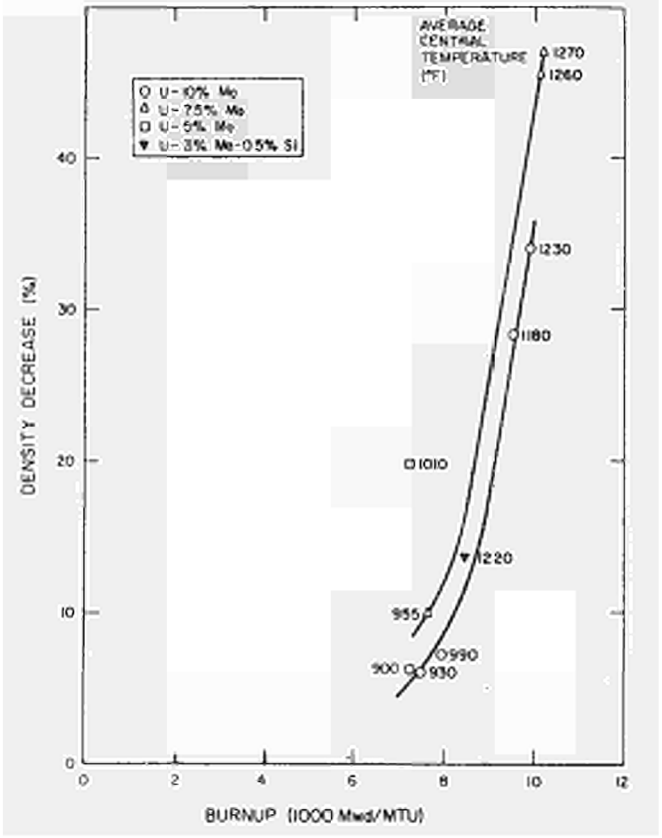

Fig. 28 - Amount of swelling as a function of burn-up, from JOHNSON and HOLLAND (ref. 40).

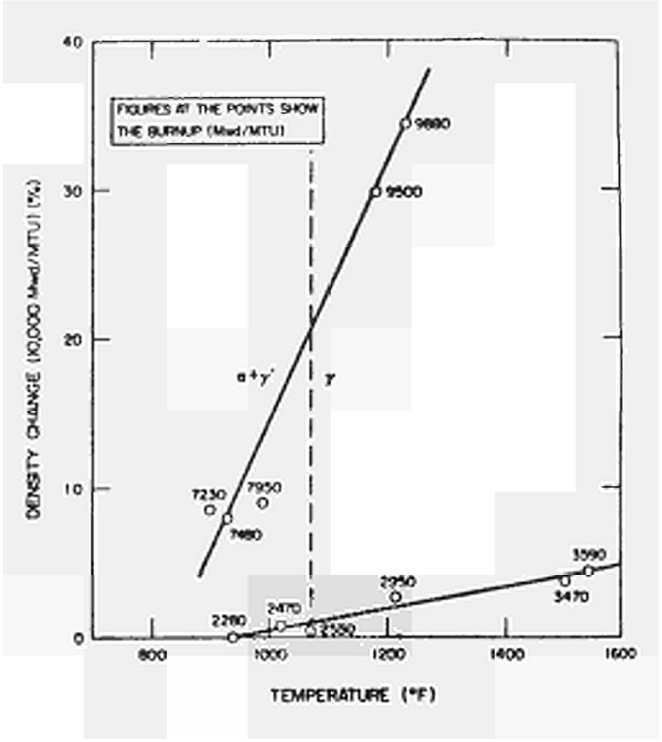

Fig. 29 - Density change versus temperature for U-10 wt% Mo alloy, from JOHNSON and HOLLAND (ref. 40).

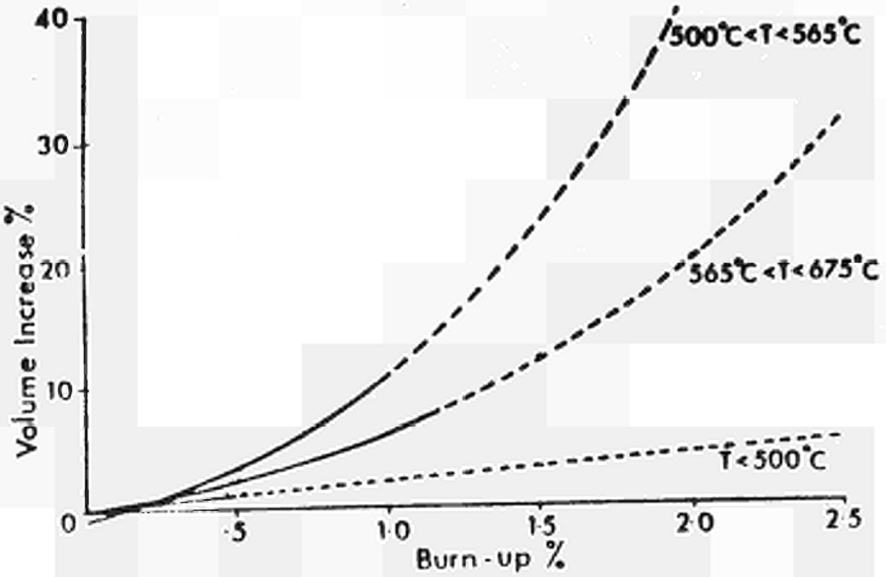

Fig. 30 - Volume increase of U - 9 wt% Mo fuel with burn-up, from PHILLIPS (ref. 42).

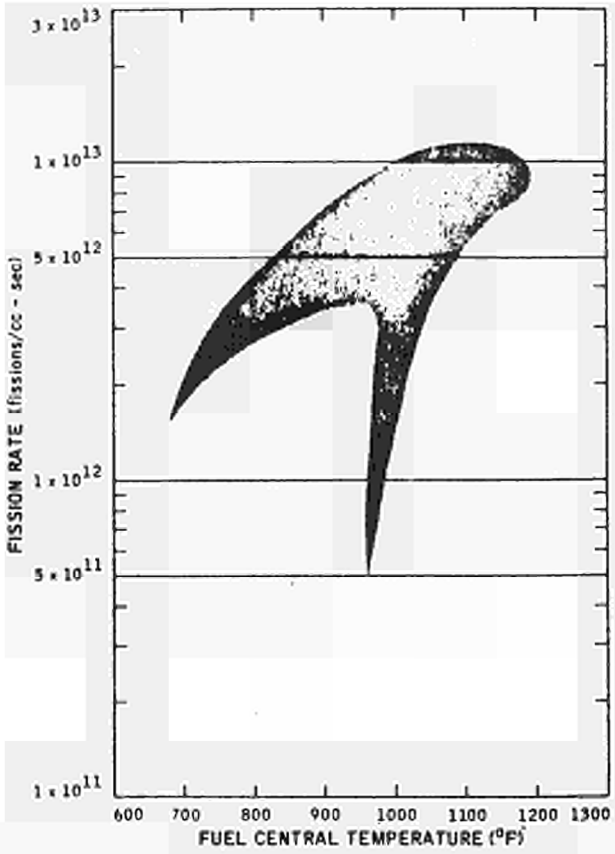

Fig. 31 - Range of temperature and fission rate conditions for HNPF Core I U - 10 wt% Mo fuel, from SCHMITT et al. (ref. 43).

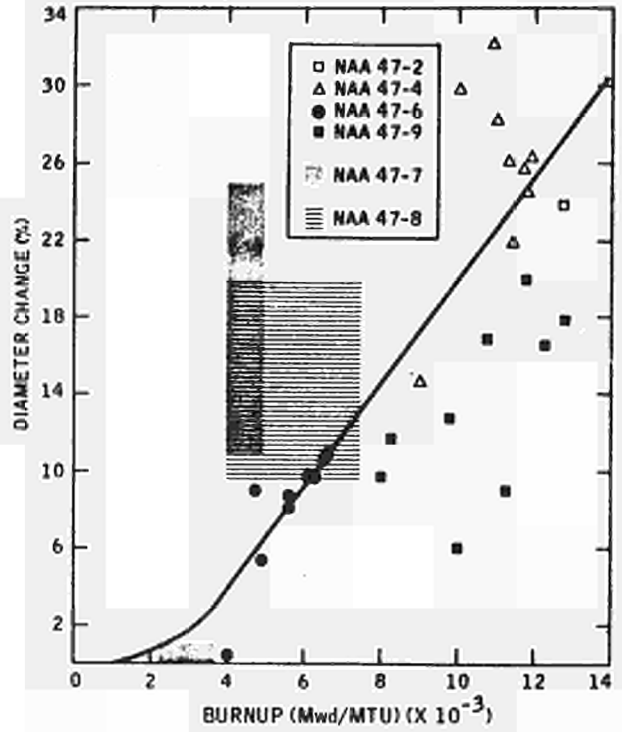

Fig. 32 - Variation of diameter change with burn-up in NAA 47 experiments, from SCHMITT et al. (ref. 43).

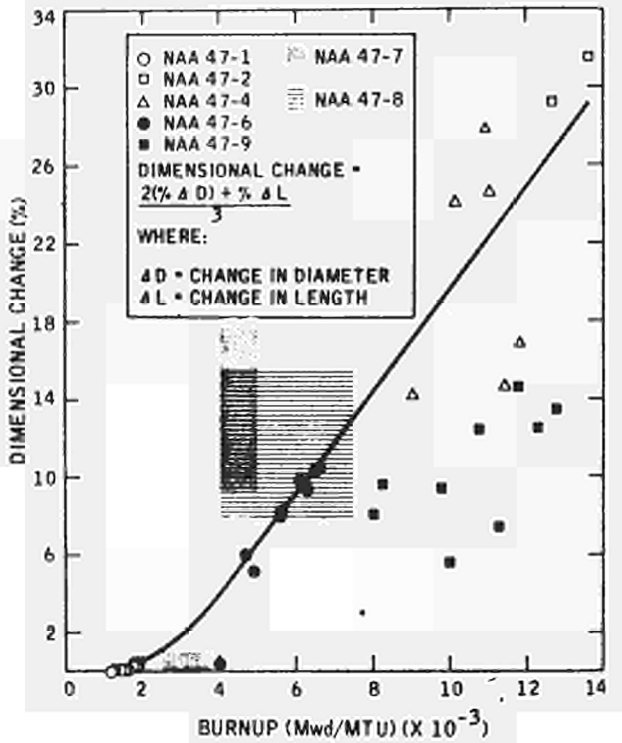

Fig. 33 - Variation of dimensional change with burn-up in NAA 47 experiments, from SCHMITT et al. (ref. 43).

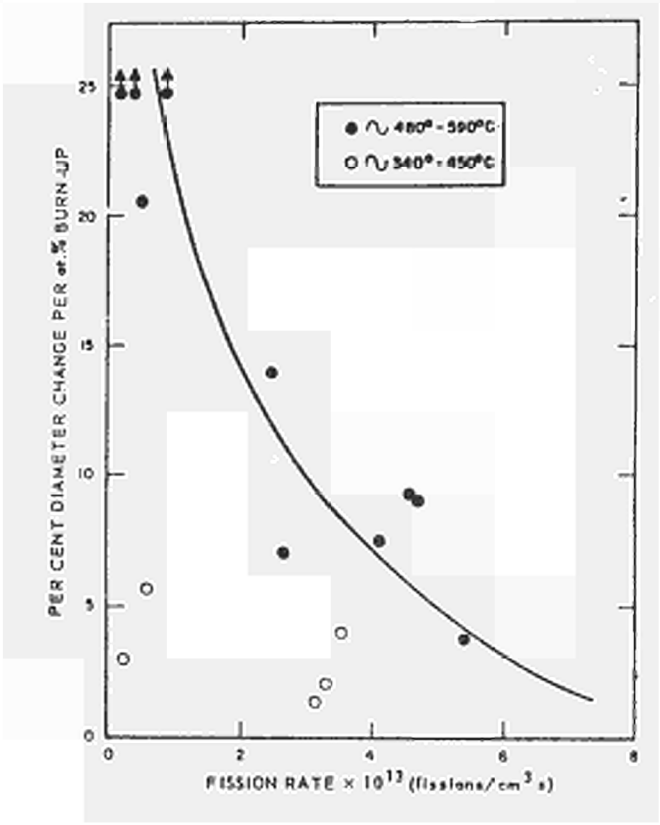

Fig. 34 - Effect of fission rate on the swelling of U - 10 wt% Mo alloy rods, from KITTEL et al. (ref. 44).

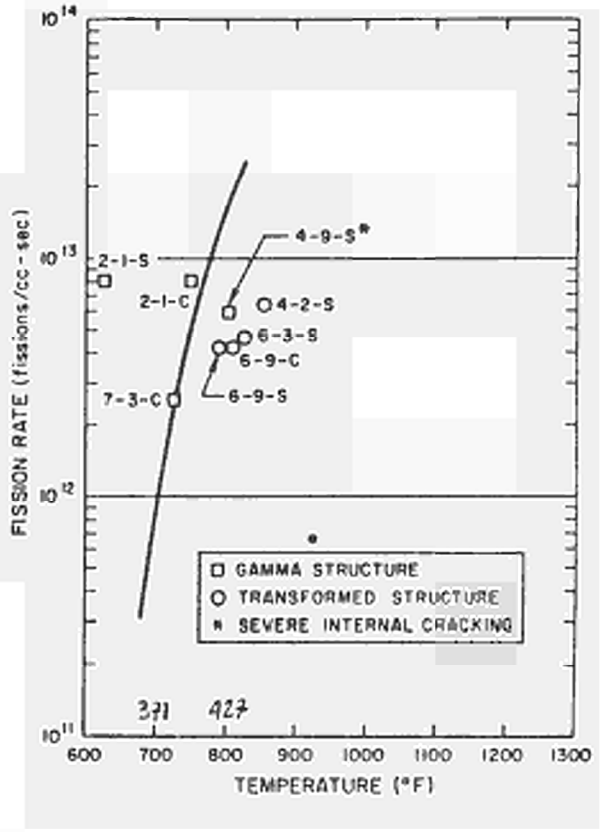

Fig. 35 - Correlation of observed microstructure with theoretical fission rate temperature curve, from WILLARD and SCHMITT (ref. 45).

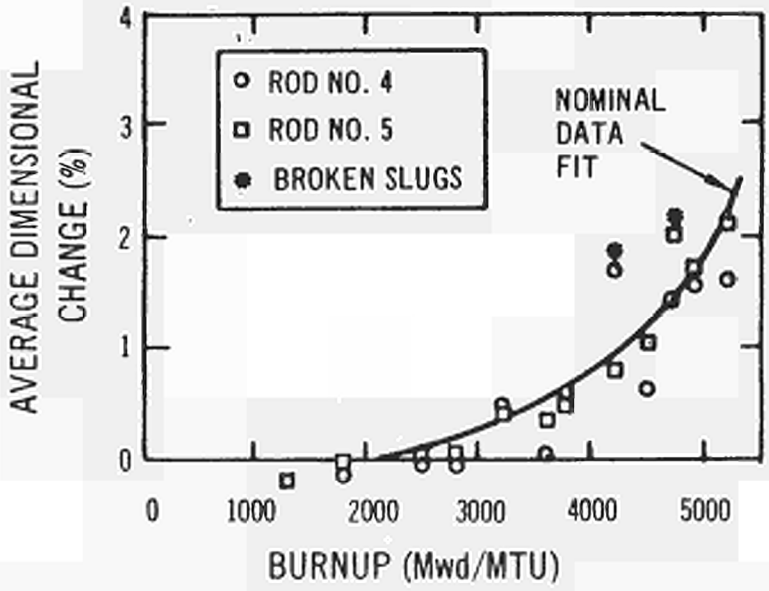

Fig. 36 - Dimensional change data for U - 10 wt% Mo fuel slugs from Su-9 experiments, from ARNOLD et al. (ref. 47).

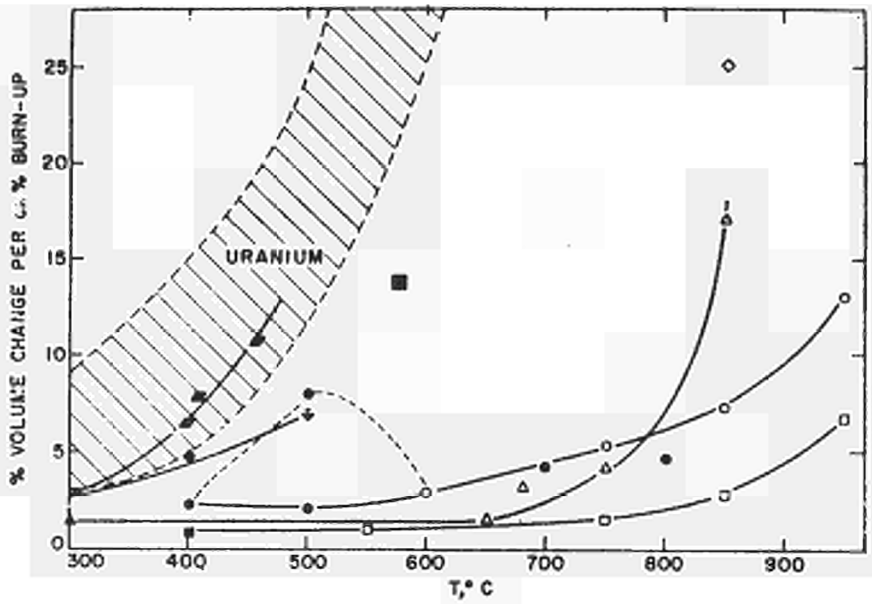

Fig. 37 - Comparison of irradiation results. Closed symbols indicate irradiation at temperature; open symbols indicate post-irradiation annealing, (ref. 51)

Data Points		Alloy
□	■	U - 10% Mo - 0.04% Sn
o	●	U - 10% Mo
△	▲	U - 4% Mo - 0.1% Si
	◆	U - 3.5% Mo - 0.1% Si
	◆	U - 4% Mo
◇		U - 4% Mo
	▨	adjusted uranium

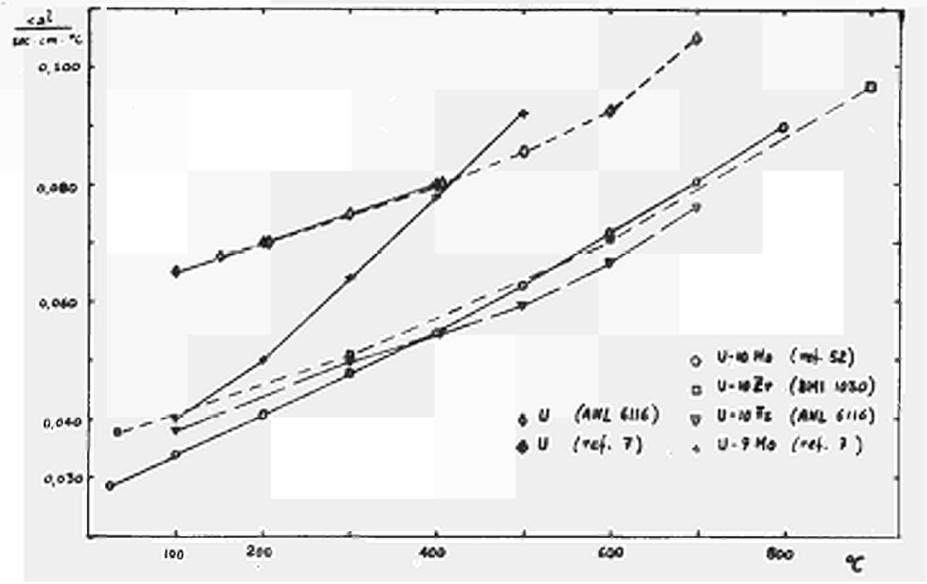

Fig. 38 - Thermal conductivity data versus temperature for different uranium alloys.

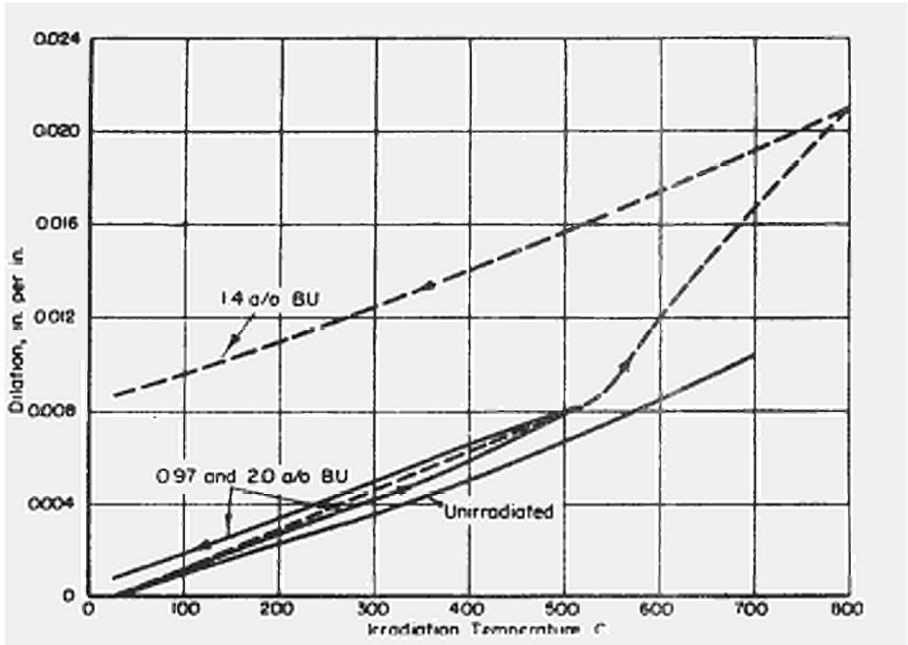

Fig. 39 - Effect of irradiation on linear thermal expansion of U - 10% Mo alloy, from D. O. LEESER et al. (ref. 34).

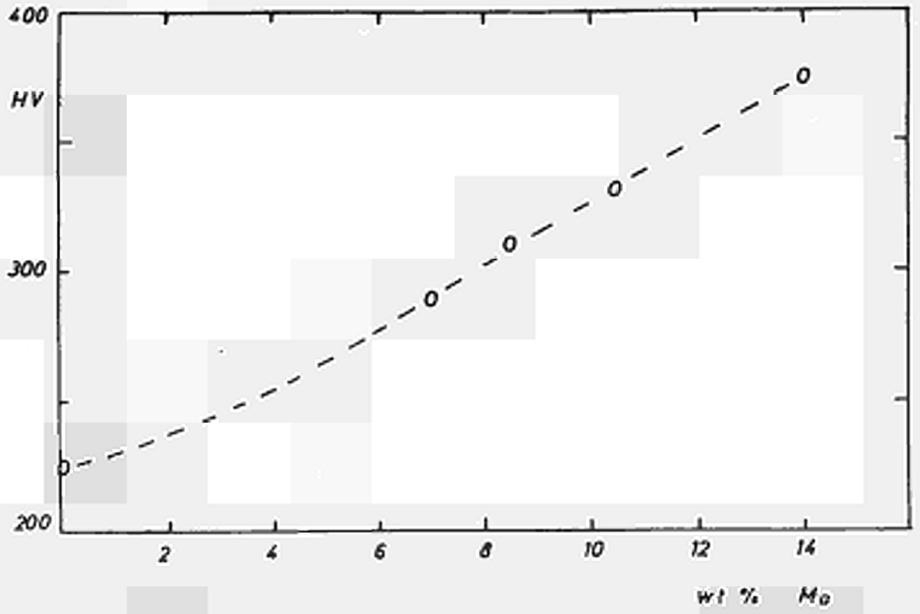

Fig. 40 - Vickers hardness at room temperature for U - Mo alloys treated 900°C - 7 days, then water quenched - ref. 56.

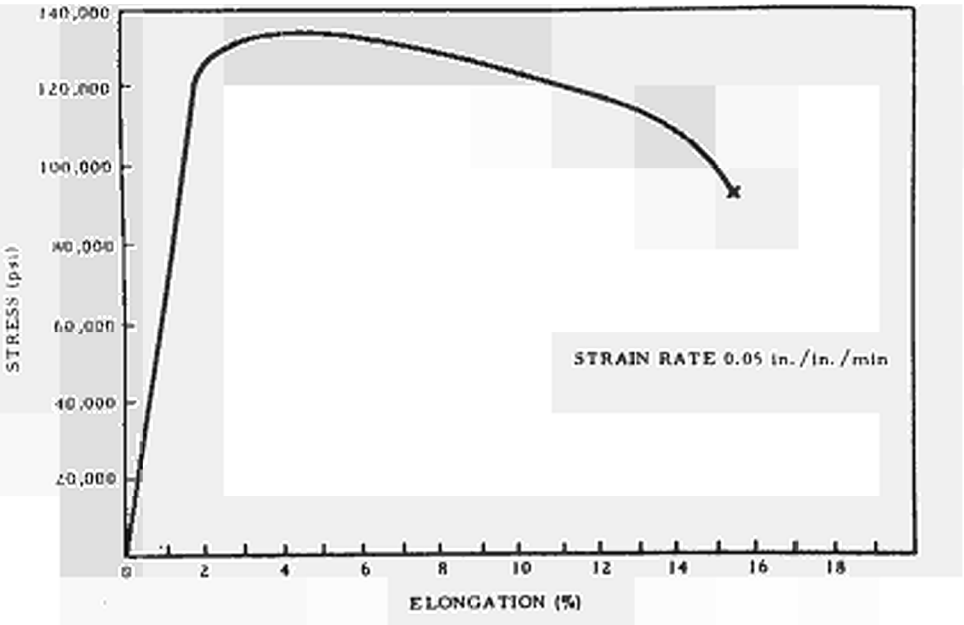

Fig. 41 - Engineering stress-strain curve for U - 10 wt% Mo alloy, from M. B. WALDRON et al., ref. 57.

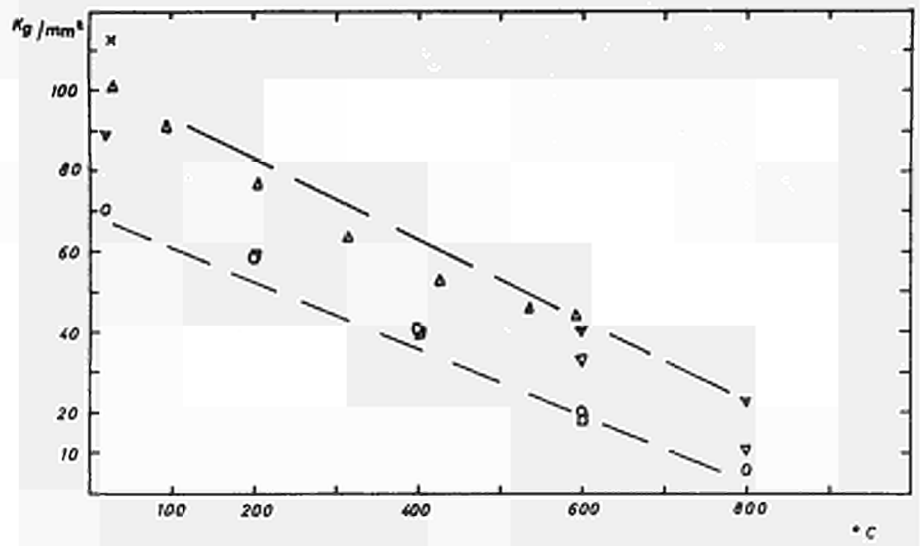

Fig. 42 - Ultimate tensile strength of gamma quenched U - 10% Mo alloys as a function of the temperature;
o - ref. 57 □ - ref. 1 × - ref. 59
△ - ref. 52 ▽ - ref. 55 (10.5% Mo)

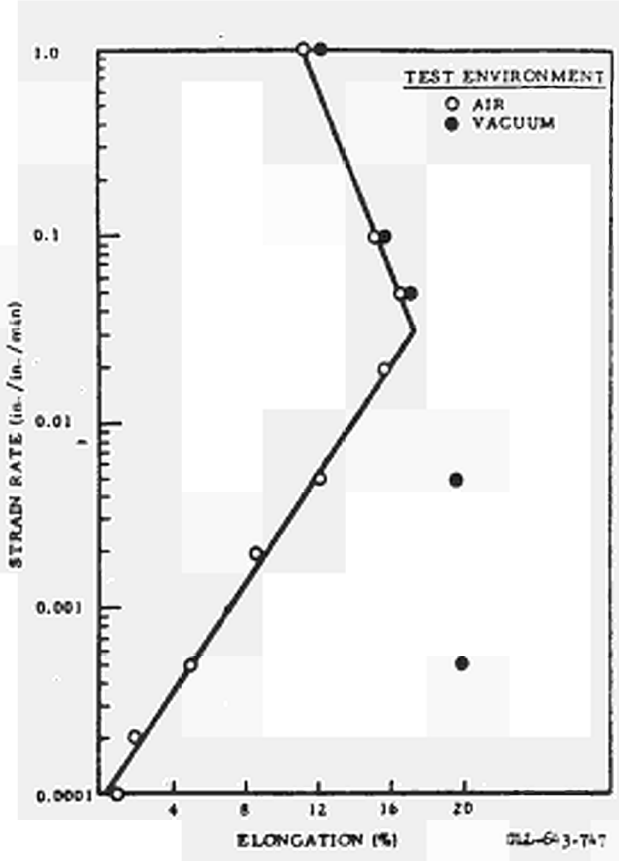

Fig. 43 - The effect of strain rate on ductility for U - 10% Mo alloy, from C. A. W. PETERSON and R. R. VANDERVOORT, (ref. 58).

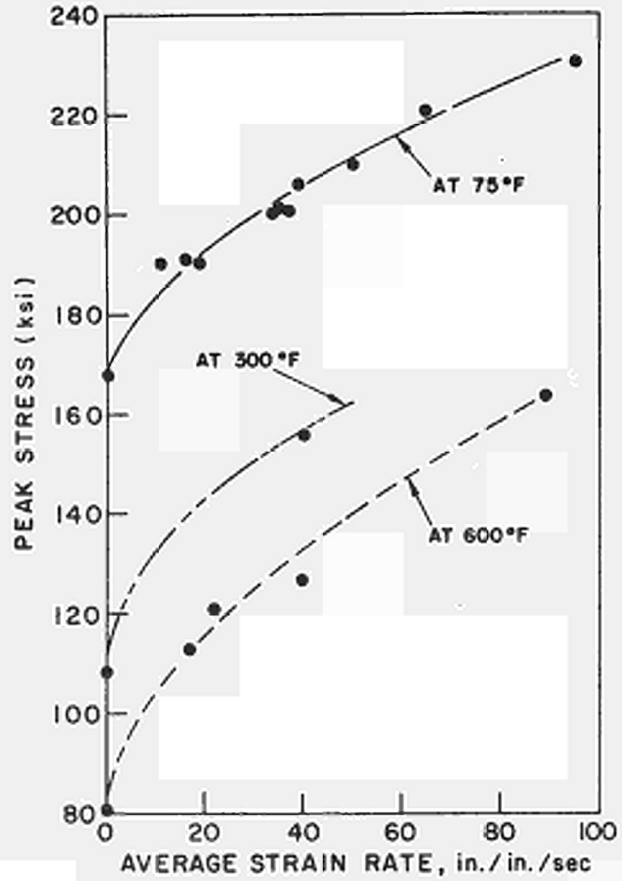

Fig. 44 - Peak stress versus strain rate for U-10% Mo alloy in extruded condition, from K. G. HOGE (ref. 62)

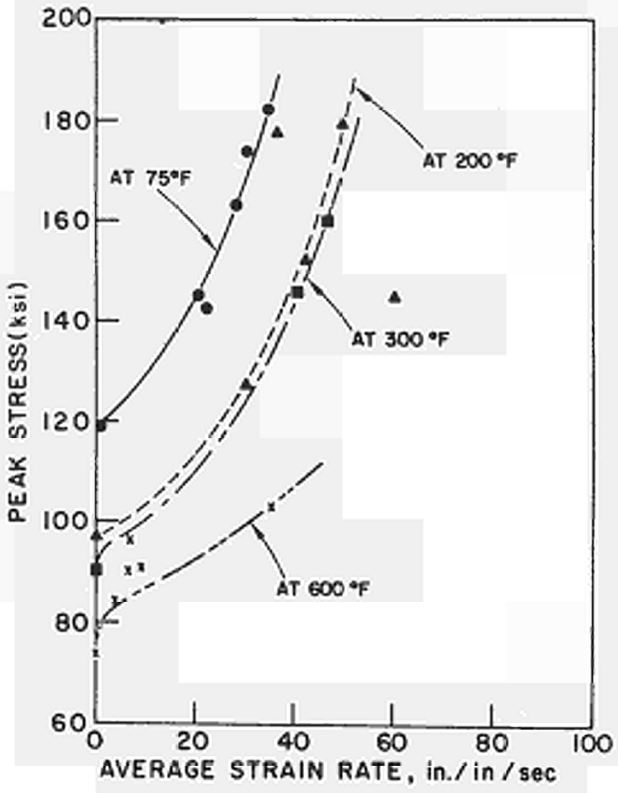

Fig. 45 - Peak stress versus strain rate for U-10% Mo alloy in as cast conditions with high carbon content, from K. G. HOGE (ref. 62)

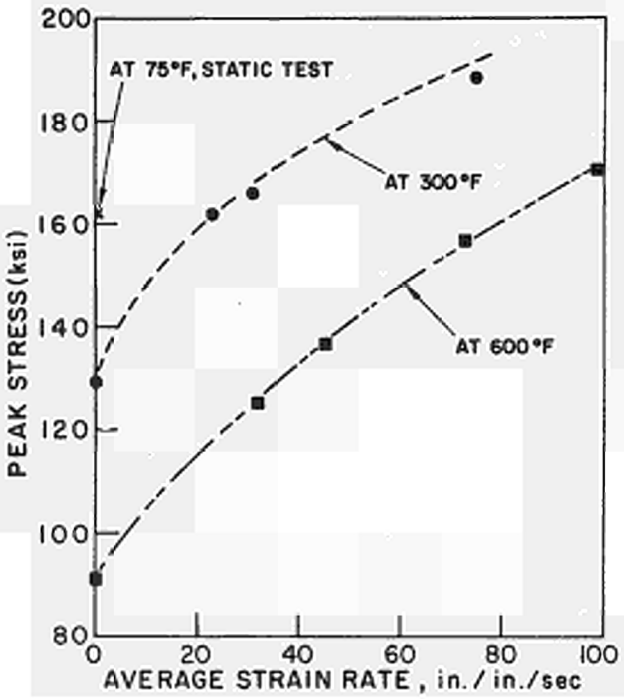

Fig. 46 - Peak stress versus strain rate for U-10% Mo alloy in hot rolled condition, from K. G. HOGE (ref. 62)

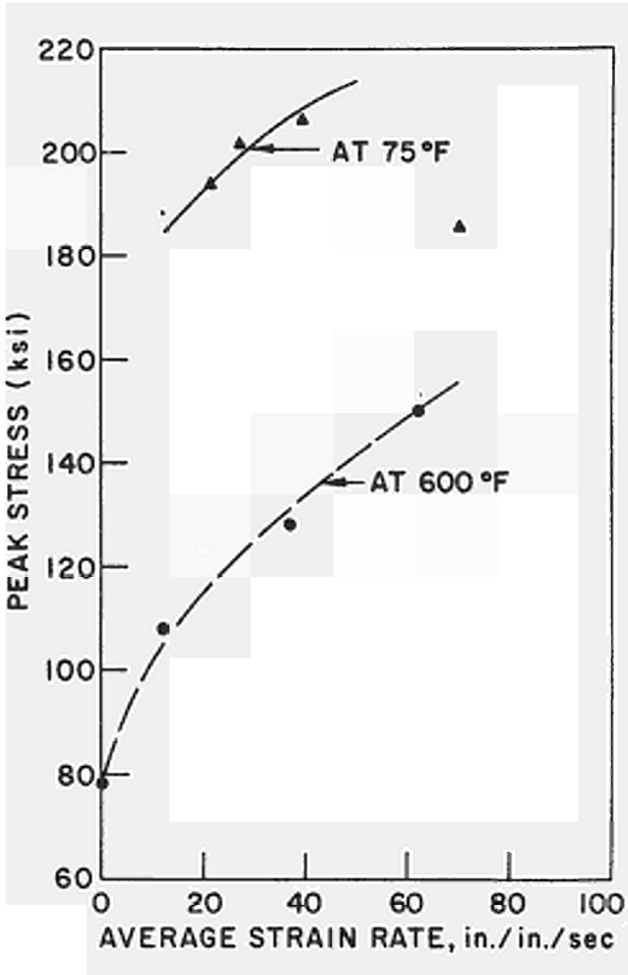

Fig. 47 - Peak stress versus strain rate for U-10% Mo alloy in as-cast condition, low carbon content, from K. G. HOGE (ref. 62)

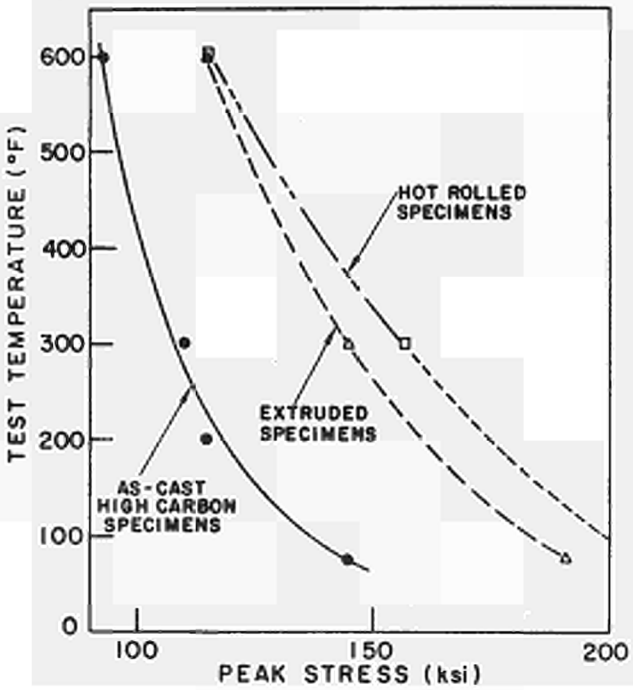

Fig. 48 - Peak stress versus test temperature for a constant strain rate of 20 in/in/sec for U-10% Mo, from K. G. HOGE -(ref. 62)

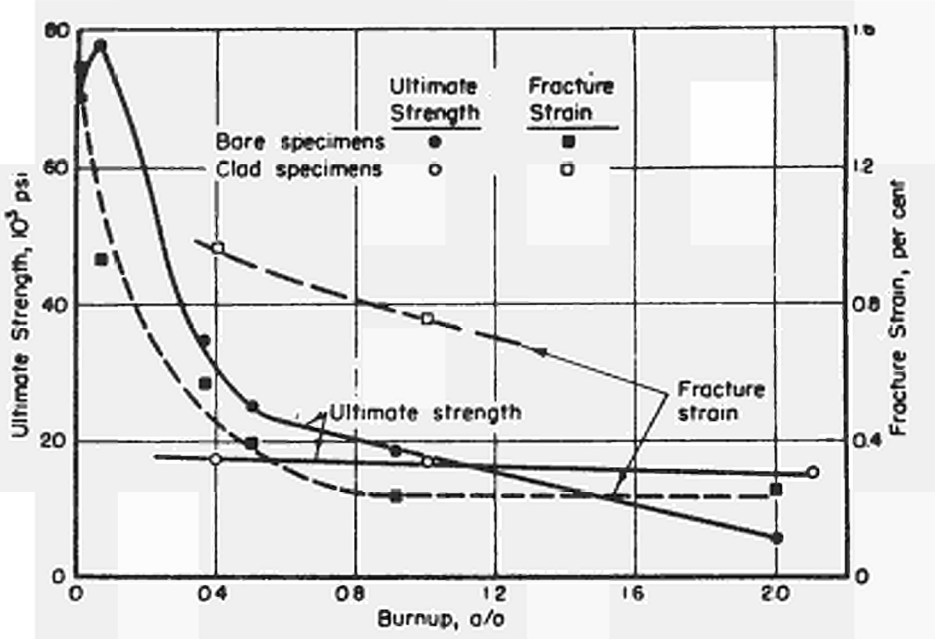

Fig. 49 - Effect of burn-up on post-irradiation ultimate strength and fracture strain of U-10% Mo alloy, measured at 500°C, from D. O. LEESER et al. (ref. 34)

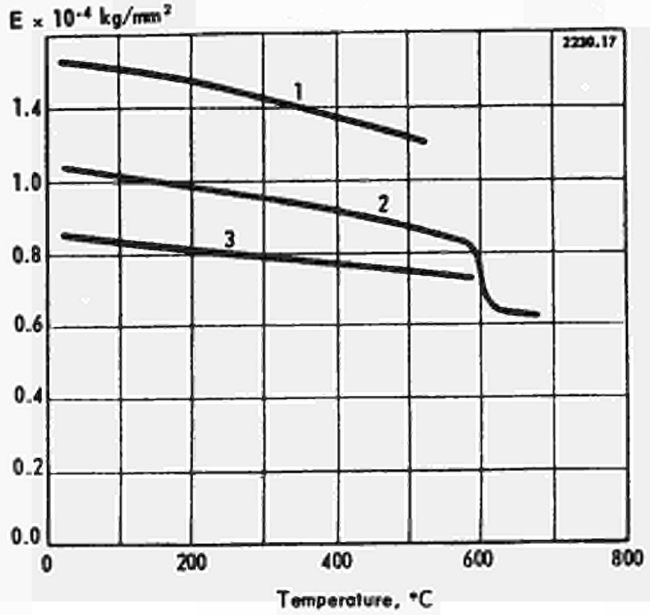

Fig. 50 - Temperature dependence of the Young's modulus of U-9 wt% Mo alloy, from S. T. KONOBEEVSKY et al. (ref. 7) - 1) after 100 hr annealing at 500°C
2) after 11 hr annealing at 520°C
3) after gamma annealing

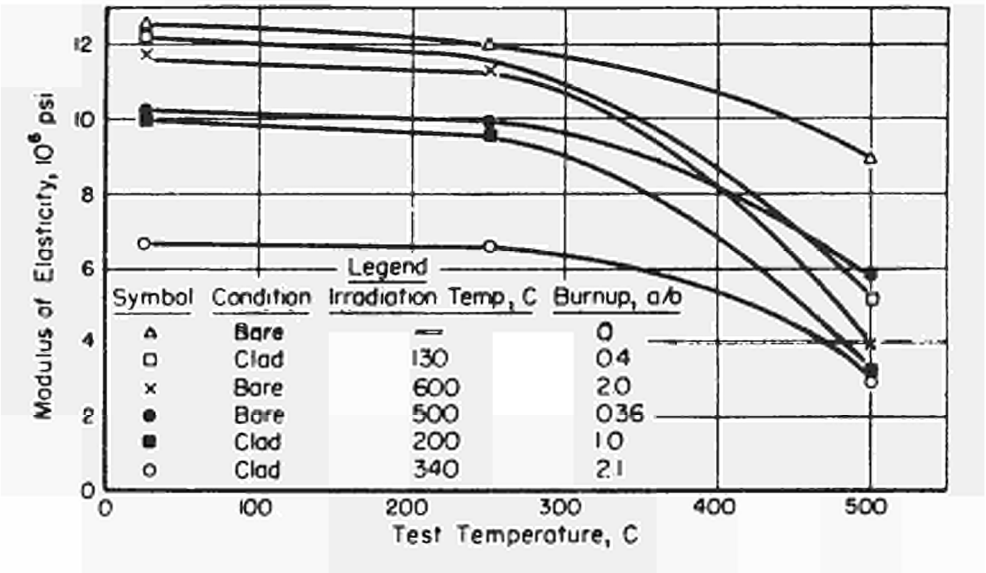

Fig. 51 - Effect of burn-up and temperature on post-irradiation elastic modulus of U-10% Mo alloy, from D. O. LEESER et al. (ref. 34)

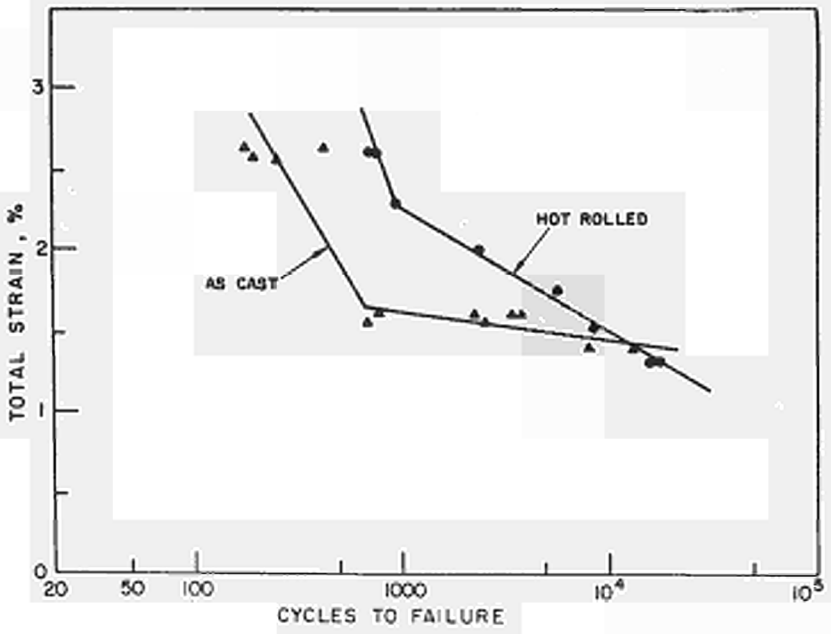

Fig. 52 - Modified S - N diagram for U-10% Mo alloy in as cast and hot-rolled conditions, from K. G. HOGE (ref. 62)

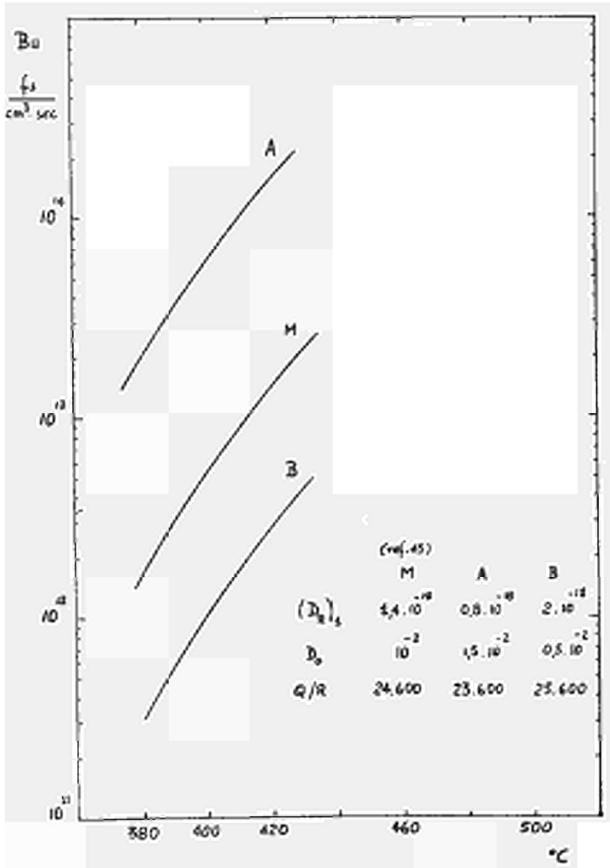

Fig. 53 - Critical fission rate as a function of the temperature: changes of the values calculated for different increases or decreases of the variables.

REFERENCES

(1) GITTUS, J.H., "Uranium", London Butterworths (1963)

(2) LARRIMORE, J.A., et al., "The SORA Reactor: design status report", Seminar on intense neutron source, USAEC-ENEA, Santa Fe, New Mexico, (Sept. 1966)

(3) BAUER, A.A., and ROUGH, F.A., "Constitution of uranium and Thorium alloys", BMI-1300 (1958)

(4) DWIGHT, A.E., "The Uranium-Molybdenum equilibrium diagram below 900°C" J. Nucl. Mat., 2, 1 (1960) 81

(5) THOMAS, D.E., et al., "Properties of gamma phase alloys of Uranium", Int. Geneva Conference 1958. Paper P/1924

(6) LEHMANN, J. and HILLS, R.F., "Proposed nomenclature for phases in uranium alloys", J. Nucl. Mat. 2, 3 (1960) 261

(7) KONOBEEVSKY, S.T., et al., "Some physical properties of uranium, plutonium and their alloys," Int. Geneva Conference 1958. Paper P/2230

(8) ROUGH, F.A., and BAUER, A.A., "Kinetics of transformations of gamma phase U-alloys", Progress in Nuclear Energy, Series V, 2 (1959) 460

(9) REPAS, P.E., et al, "Transformation characteristics of three Uranium base alloys", Report AMRA/CR-63-02/1F January 1963

(10) SALLER, H.A., ROUGH, F.A. and BAUER, A.A., "Report BMI-957, October 1954

(11) McGEARY, R.K., "Development and properties of Uranium-base alloys resistant in high temperature water", USAEC Report WAPD-127 - Part I. Alloys without protective cladding. (April 1955)

(12) VAN THYNE, R.J., and McPHERSON, D.J., "Transformation Kinetics of Uranium-Molybdenum alloys", Trans. ASM, 49 (1957) 598

(13) BELLOT, J., DOSIERE, P. and HENRY, J.M., "Etude des alliages Uranium-Molybdène métaux" - September 1958, 343

(14) DONZE, G. and CABANE, G., "Mécanisme de la décomposition de la phase gamma des alliages Uranium-Molybdène et Uranium-Molybdène-Ruthénium", Mém. Scient. Rev. Metallurg. LVII, 6 (1960) 450

(15) MIKAILOFF, H., "Etude des transformations par revenu de la phase gamma cubique centrée des alliages Uranium-Molybdène", Rapport C.E.A. No. 1270 (1960)

(16) HOLLAND, W.A., "Isothermal transformation of U-14 and U-16 wt% Mo-alloys at 550°C", Report NAA-SR-6125 (Dec. 1961)

(17) SHOUDY, A.A., McHUGH, W.E., and SILLIMAN, M.A., "The Effect of irradiation temperature and fission rate on the radiation stability of Uranium - 10 wt% Molybdenum alloy","Radiation Damage in reactor materials", IAEA - Vienna 1963, p. 133

(18) PETERSON, C.A.W., STEELE, W.J., DIGIALLONARDO, S.L., "Isothermal transformation study of some Uranium-base alloys", Report UCRL-7824 (August 1964)

(19) BAR-OR, A., et al., "Uranium alloys", Int. Geneva Conference 1964 - Paper P/150

(20) REPAS, P.E., GOODENOW, R.H., and HEHEMANN, R.F., "Transformation characteristics of U-Mo and U-Mo-Ti alloys", Trans. ASM 57 (1964) 150

(21) GOLDSTEIN, Y. and BAR-OR, A., "Decomposition of gamma phase in Uranium alloys containing 8, 10.8 and 14.3 wt% Molybdenum", J. Inst. Metals 95 (1967) 17

(22) SALLER, H.A., DICKERSON, R.F. and HURR, W.E., "Uranium alloys for high temperature application", Report BMI-1098 (1956)

(23) BODZIN, J.J., "Thermal cycling experiments on blanket elements and fuel pins to determine the effect of cycling in the alpha-plus-epsilon phase on physical size and microstructure", Report NP 9131 (March 1960)

(24) KOVACIC, E.C., McHUGH, W.E., and SHOUDY, A.A., "Materials problems and selections in the Enrico Fermi fast breeder reactor", Nucl. Metallurgy IX, Materials forSodium-Cooled Reactors-ANS's 1963 Winter Meeting, p. 115

(25) MINUSHKIN, B., "Thermal cycling tests on U-10 Mo for the ORNL Fast burst reactor", Report NDA-Memo-2136 (July 1960)

(26) BOLTAX, A., "Behaviour of fissionable material under irradiation", "Nuclear Reactor Fuel Elements", ed., by A.R. Kaufmann 1962, Chapter 9, p. 292

(27) KONOBEEVSKY, S.T., et al., "Effect of irradiation on structure and properties of fissionable materials", Int. Geneva Conference 1955 - Paper P/681

(28) KONOBEEVSKY, S.T. et al., "Structural changes occurring in fissile materials during irradiation", Int. Geneva Conference 1958 - Paper P/2192

(29) BLEIBERG, M.L. et al., "Phases changes in pile-irradiated Uranium-base alloys", J. Appl. Phys. 27 (1956) 1270

(30) BLEIBERG, M.L., "Irradiation-induced phase changes in Uranium-base alloys", Int. Geneva Conference 1958 - Paper P/619

(31) CALKINS, G.D., et al., "Radiation stability studies on binary uranium alloys", 2nd Nuclear Engineering and Science Conf. Paper 57 - NESC - 109 (March 14, 1957)

(32) CALKINS, G.D. et al., "Effect of heat treatment and burn-up on radiation stability of Uranium-10 wt% Molybdenum fuel alloys", ASTM Special Technical Publication No. 220 (Febr. 1958)

(33) DEL GROSSO, A. and LEESER, D.O., "The APDA test program on selected Uranium fuel alloys, June 1954 - June 1957", Report APDA-122 (1959)

(34) LEESER, D.O., ROUGH, F.A. and BAUER, A.A., "Radiation Stability of fuel elements for the Enrico Fermi Power Reactor", Int. Geneva Conference 1958 - Paper P/622

(35) BLEIBERG, M.L. et al., "Development and properties of Uranium-base alloys resistant in high temperature water", Report WAPD - 127, Part IV - Radiation stability of Uranium-base alloys, May(1957)

(36) HUEBOTTER, P.R., SHOUDY, A.A., "Summary and evaluation of irradiation data on U-10 wt% Mo fuel alloys as of April 12, 1960 MAT. - 759, Memo

(37) "Irradiation studies of U-10 wt% Mo fuel alloy", BMI-APDA-660 January 1961

(38) BLESSING, W.G. et al., " Summary of the APDA fuel development programs" Report APDA-143-April 1961

(39) SILLIMAN, M.A., et al., "Irradiation testing of Enrico Fermi Prototype fuel pins in the CP-5'Report APDA-130 (1960)

(40) JOHNSON, M.P. and HOLLAND, W.A., "Irradiation of U-Mo base alloys" Report NAA-SR-6262 - January 1964

(41) COTTRELL, S.A., "Development and performance of Dounreay fast reactor metal fuel", Int. Geneva Conference, 1964 - Paper P/150

(42) PHILLIPS, J.L., "Full power operation of the Dounreay fast Reactor", Report ANS-100 (1965) 7

(43) SCHMITT, A.R., WILLARD, R.M. and MAGNUS, D.K., "The NAA 47 U-10 Mo fuel irradiation program for HNPF Core 1", Report NAA-SR-8955 (February 1965)

(44) KITTEL, J.H. et al., "Irradiation behaviour of metallic fuels", Int. Geneva Conference, 1964 - Paper P/239

(45) WILLARD, R.M. and SCHMITT, A.R., "Irradiation swelling, phase reversion and intergranular cracking of U-10 wt% fuel alloys", Report NAA-SR-8956 (February 1965)

(46) BLEIBERG, M.L., "Effect of fission rate and lamella spacing upon the irradiation-induced phase transformation of U-9 wt% Mo alloy", J. Nucl. Mat. 2 (1959) 182

(47) ARNOLD, J.L., MILLER, K.J., PETERSON, R.M., "U-10 wt% Mo fuel element - irradiation in SRE", Report NAA-SR-11121 (Aug. 1965)

(48) DMITRIEV, V.D., IBRAGIMOV, SH. SH., KARMILOV, A.G., "Influence of neutron irradiation on structure and properties of Uranium alloys with 0.6 ÷ 9 wt% of Molybdenum", Atomnaya Energiya 22, 6 (1967) 459

(49) BARNES, R.S., et al., "The irradiation behaviour of Uranium and Uranium alloy fuels", Int. Geneva Conference 1964, Paper P/145

(50) KRAMER, D. and JOHNSTON, W.V., "Post-irradiation annealing of U-Mo ternary alloys", J. Nucl. Mat. 9, 2 (1963) 213

(51) KRAMER, D., JOHNSTON, W.V. and RHODES, C.G., "Reduction of fission-product swelling in Uranium alloys by means of finely dispersed phases", J. Inst. Metals 93 (1964-65) 145

(52) KLEIN, J.L., "Uranium and its alloys","Nuclear Reactor fuel elements", ed. by A.R. Kaufmann 1962 - Chapter 3, p. 31

(53) STATHOPLOS, A., "Preliminary design of the ORNL fast burst reactor", Report NDA-2136-1 (July 1960)

(54) FARKAS, M.S., "Mechanical and physical properties of fuels and cladding materials with potential for use in Brookhaven's pulsed fast reactor", Report BMI-X-455 (July 1967)

(55) PETERSON, C.A.W., VANDERVOORT, R.R., "Mechanical Properties of some Uranium alloys", Report UCRL-7771 (1964)

(56) BOUDOURESQUES, B. and ENGLANDER, M., "Strength and creep of Uranium alloys", Progress in Nuclear Energy - Series V, 2 (1959) 621

(57) WALDRON, M.B., BURNETT, R.C. and PUGH, S.F., "The mechanical properties of Uranium-Molybdenum alloys", Report AERE-M/R -2554 (1958)

(58) PETERSON, C.A.W. and VANDERVOORT, R.R. "Stress cracking in the Uranium-10 wt% Molybdenum alloy", Report UCRL-7767 (March 1964)

(59) HILLS, R.F., BUTCHER, B.R. and HOWLETT, B.W., "The Mechanical properties of quenched Uranium-Molybdenum alloy - Part I", J. Nucl. Mat. 11, 2 (1964) 149

(60) WILKINSON, W.D., "Uranium Metallurgy - Vol. II" Chapter 8, Uranium alloys, Interscience Publishers 1962

(61) RIENECKER, F. and MORAN, W.H., "Uranium-Molybdenum Alloy for use in a prompt-burst reactor", J. of Basic Engineering 12 (1965) 865

(62) HOGE, K.G., "Some mechanical properties of U-10% Mo alloy under dynamic tension loads", J. of Basic Engineering 6 (1966) 509

(63) GATES, J.E. et al., "Stress strain properties of irradiated Uranium-10 wt% Molybdenum", Report BMI-APDA-638 (Jan. 1958)

(64) SALLER, H.A. et al., "Creep strength of Uranium alloys", Report BMI-834 (May 1953)

APPENDIX A
CONVERSION UNITS

1 psi	=	0.07031	kg/cm^2
1 kg/cm^2	=	14.223	psi
1x10^3 psi	=	0.7031	kg/mm^2
1 kg/mm^2	=	1422.3	psi
1 tonn (2240 pound)/in^2	=	1.5749	kg/mm^2
1 kg/mm^2	=	0.6349	$tonn/in^2$
1 kg/mm^2	=	9.8066x10^7	$dynes/cm^2$

1 $cal/(cm^2$-sec-^oC/cm) = 0.8060 Btu/(sq. foot-sec-^oF/in)

1 Btu/lb-^oF = 1 cal/gr-^oC = 4.186 joules/gr-^oC

Temperature conversion:

^oC	^oF	^oC	^oF
20	68	400	752
37.8	100	426.7	800
93.3	200	450	842
100	212	482.2	900
148.9	300	500	932
200	392	537.8	1000
204.4	400	550	1022
260	500	593.3	1100
300	572	600	1112
315.6	600	648.9	1200
350	662	700	1292
371.1	700	760	1400
		800	1472

APPENDIX B

We consider the "critical fission rate" Bu as defined by WILLARD and SCHMITT (45) and expressed by the equation

$$Bu = \frac{(Bu)_1}{(D_R)_1} D_o \exp(-Q/RT) \qquad (\text{fissions/cm}^3\text{-sec}) \qquad (1)$$

where

D_R = radiation-induced diffusion coefficient
D_o = thermal diffusion constant
Q = activation energy for thermal diffusion
R = gas constant
T = absolute temperature

Let us consider Δx as the uncertainty of the measured and calculated values of the variable x, and ε the variation of the function $f = f(x)$ as affected by the uncertainty of the variable x; in our case ε is defined by

$$\varepsilon = \sum_1^n \left| \frac{\partial f(x_1, x_2, \ldots x_n)}{\partial x_n} \Delta x_n \right| \qquad (2)$$

and we consider Bu as f, and $(Bu)_1$, $(D_R)_1$, D_o, Q as the variables x_n. We can write, from equations (1) and (2):

$$\varepsilon = \left| \frac{\partial Bu}{\partial (Bu)_1} \Delta (Bu)_1 \right| + \left| \frac{\partial Bu}{\partial (D_R)_1} \Delta (D_R)_1 \right| + \left| \frac{\partial Bu}{\partial D_o} \Delta D_o \right| +$$
$$+ \left| \frac{\partial Bu}{\partial Q} \Delta Q \right| = \left| \frac{D_o}{(D_R)_1} \exp(-Q/RT) \cdot \Delta (Bu)_1 \right| +$$
$$+ \left| \frac{(Bu)_1}{(D_R)_1^2} \cdot D_o \exp(-Q/RT) \Delta (D_R)_1 \right| + \left| \frac{(Bu)_1}{(D_R)_1} \exp(-Q/RT) \Delta D_o \right| +$$
$$+ \left| \frac{(Bu)_1}{(D_R)_1} \frac{D_o}{RT} \exp(-Q/RT) \Delta Q \right|$$

We make now the calculation for the temperature of 400°C and with the values indicated by the above mentioned authors (45):

$(Bu)_1 = 5.25 \cdot 10^{12}$ fs/cm^3-sec
$(D_R)_1 = 1.4 \pm 0.6 \cdot 10^{-18}$ cm^2/sec

$D_o = 10^{-2}\ cm^2/sec$

$\frac{Q}{R} = 24.600\ {}^oK^{-1}$

$$\varepsilon = 0.336 \cdot \Delta (Bu)_1 + 3.6 \cdot 10^{30} \Delta (D_R)_1 + 4.9 \cdot 10^{14} \Delta D_o + 3.7 \cdot 10^9 \Delta Q$$

We make now the following assumptions for the uncertainties, based on the possible errors in the utilized values:

$\Delta (Bu)_1 = 0.05 \cdot 10^{12}\ fs/cm^3\text{-sec}$
$\Delta (D_R)_1 = 0.6 \cdot 10^{-18}\ cm^2/sec$
$\Delta D_o = 0.5 \cdot 10^{-2}\ cm^2/sec$
$\Delta Q = 1 \cdot 10^3\ cal/mol$

With these assumptions, ε is the addition of these factors

$(Bu)_1 \longrightarrow 0.017 \cdot 10^{12}$
$(D_R)_1 \longrightarrow 2.16 \cdot 10^{12}$
$D_o \longrightarrow 2.5 \cdot 10^{12}$
$Q \longrightarrow 3.7 \cdot 10^{12}$

$$\varepsilon \simeq 8.4 \cdot 10^{12}.$$

Bu = $4.8 \cdot 10^{12}\ fs/cm^3$-sec for T = 400°C; with the above mentioned assumptions, the variation of Bu, calculated as ε, is very high. The variables which have more influence on the Bu-values are $(D_R)_1$, D_o and Q; the curve of the critical fission rate may be deplaced of an order of magnitude by the errors in the values of the variables. A graphical comparison of the curves calculated with different values is indicated in fig. 53.
Consequently, when the irradiation conditions are in the critical range, it is very important to know the uncertainties of the utilized values.

NOTICE TO THE READER

All Euratom reports are announced, as and when they are issued, in the monthly periodical **EURATOM INFORMATION**, edited by the Centre for Information and Documentation (CID). For subscription (1 year : US$ 15, £ 6.5) or free specimen copies please write to :

Handelsblatt GmbH
"Euratom Information"
Postfach 1102
D-4 Düsseldorf (Germany)

or

Office central de vente des publications
des Communautés européennes
2, Place de Metz
Luxembourg

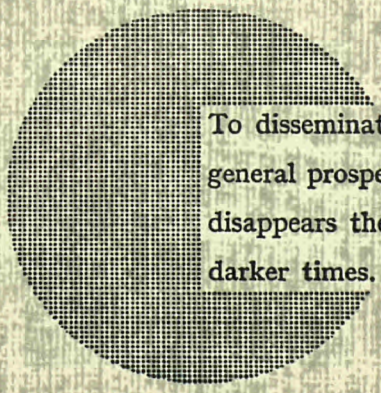

To disseminate knowledge is to disseminate prosperity — I mean general prosperity and not individual riches — and with prosperity disappears the greater part of the evil which is our heritage from darker times.

Alfred Nobel

SALES OFFICES

All Euratom reports are on sale at the offices listed below, at the prices given on the back of the front cover (when ordering, specify clearly the EUR number and the title of the report, which are shown on the front cover).

OFFICE CENTRAL DE VENTE DES PUBLICATIONS DES COMMUNAUTES EUROPEENNES
2, place de Metz, Luxembourg (Compte chèque postal N° 191-90)

BELGIQUE — BELGIË
MONITEUR BELGE
40-42, rue de Louvain - Bruxelles
BELGISCH STAATSBLAD
Leuvenseweg 40-42 - Brussel

DEUTSCHLAND
BUNDESANZEIGER
Postfach - Köln 1

FRANCE
SERVICE DE VENTE EN FRANCE
DES PUBLICATIONS DES
COMMUNAUTES EUROPEENNES
26, rue Desaix - Paris 15e

ITALIA
LIBRERIA DELLO STATO
Piazza G. Verdi, 10 - Roma

LUXEMBOURG
OFFICE CENTRAL DE VENTE
DES PUBLICATIONS DES
COMMUNAUTES EUROPEENNES
9, rue Goethe - Luxembourg

NEDERLAND
STAATSDRUKKERIJ
Christoffel Plantijnstraat - Den Haag

UNITED KINGDOM
H. M. STATIONERY OFFICE
P. O. Box 569 - London S.E.1

EURATOM — C.I.D.
51-53, rue Belliard
Bruxelles (Belgique)